National Technical University of Athens

Translational Engineering in Health and Medicine

Dissection mechanics of tissue components in human aorta

M.Sc. Thesis

Eleni Papanikolaou

Supervisor: Christos Manopoulos, Assist. Professor

October 2024

Contents

Summary 5

Abstract 7

Introduction 8

Thoracic Aortic Aneurysms 8

Definition 8

Prevalence 9

Risk Factors, associations, and causes 9

Aortic Dissection 11

Definition 11

Prevalence 11

Assessment of Aortic Dimensions for Risk Stratification 12

Pathogenesis 13

Classification 14

Diagnosis 14

Clinical Features 14

Prediction Methods 15

Treatment 15

Follow-Up and Surveillance 16

Mental Health Impact 16

Aortic Wall Structure 17

Biomechanics of aorta 18

Literature Review 20

Methodology 22

Material 22

Specimen Preparation 22

Mechanical Testing 26

Device 26

Direct Tension Test Protocol 27

Analysis 28

Strength of materials 28

Processing Of Experimental Data 30

Results 36

Comparison between layers and anatomical regions 38

Force - Displacement Curves 38

Yield Force (F_{yield}) 42

Elastic Modulus 43

Maximum Force (F_{max}) 44

Peak Elastic Modulus (PEM) 45
Stretch 46
Stress and strain behavior 48
Patients' characteristics influence on mechanical properties 50
Patients' characteristics influence on thickness 52
Discussion 54
Conclusion 56
References 57

Summary

The study of the mechanical properties of the aneurysmatic ascending aorta is of significant clinical and scientific interest due to the critical role of this major blood vessel in systemic circulation and the severe consequences that arise from its failure. Aneurysms of the ascending aorta can lead to life-threatening conditions such as aortic dissection and rupture. Understanding the mechanical behavior of the aorta, especially how it fails under various mechanical stresses, is essential for predicting rupture risk and improving therapeutic interventions. The focus of this research is the examination of the mechanical properties of the aortic wall under radial tensile stress, specifically to explore how different layers of the aortic wall respond to rupture propagation. The research question that guides this study is: how do the mechanical properties of the aneurysmatic ascending aorta differ between the inner (intima-media) and outer (media-adventitia) layers across various anatomical regions, and what implications do these differences have for rupture risk in patients with aortic aneurysms?

This study uses direct tension tests to investigate the radial mechanical properties of coin-shaped specimens derived from the aneurysmatic ascending aortas of twelve patients. The specimens were taken from four distinct anatomical regions of the aorta (anterior, right lateral, posterior, and left lateral) and were tested under two conditions: one set of specimens had an initial incision between the intima and media layers (inner incision), while the other set had an incision between the media and adventitia layers (outer incision). The purpose of these incisions was to simulate rupture initiation at different layers of the aortic wall, with the aim of understanding how the rupture propagates in each case. The radial tensile testing method was selected because it directly evaluates the strength of interlamellar connections within the aortic wall, particularly between the layers that are most susceptible to dissection and rupture in pathological conditions.

The data collected from the tension tests were primarily force-displacement curves for each specimen, which allowed for the calculation of several key mechanical parameters, including maximum force (F_{max}), yield force (F_{yield}), strain, and elastic modulus. These parameters were analyzed to characterize the mechanical behavior of the aortic wall in both the elastic and plastic regions of deformation, providing insight into how the wall withstands mechanical stress and the conditions under which it fails. For each anatomical region and incision type, average force-displacement curves were generated, and these curves were used to extract the relevant mechanical data. The data were then compared across the different regions and layers, and were interpreted in relation to existing literature on aortic mechanics, particularly studies that have examined the radial tensile properties of the aorta.

The results of the study reveal several important findings regarding the mechanical behavior of the aneurysmatic ascending aorta. One of the key observations is that specimens with inner incisions, which mimic rupture initiation between the intima and media layers, consistently exhibited higher maximum forces at failure (F_{max}) compared to specimens with outer incisions, where rupture initiation occurred between the media and adventitia layers. This suggests that the inner layers of the aortic wall, particularly the intima-media interface, possess greater mechanical strength and resistance to rupture than the outer layers. These findings are consistent with the results of previous studies, such as those by Sommer et al. and Schriefl et al., which have reported lower mechanical resistance in the outer layers of the aortic wall due to weaker interlamellar connections. The higher F_{max} values observed in the inner layers indicate that these layers play a critical role in maintaining the mechanical stability of the aorta under tensile stress, while the outer layers are more prone to rupture.

The study also found significant differences in mechanical performance between the various anatomical regions of the aorta. The posterior and right lateral regions consistently exhibited higher mechanical resistance, with greater F_{max} and elastic modulus values, compared to the anterior and left lateral regions. This suggests that the structural integrity of the aortic wall varies depending on its anatomical location, with certain regions being more mechanically robust than others. The posterior region, in particular, demonstrated high resistance to mechanical stress, which may be attributable to differences in the organization of collagen and elastin fibers within the aortic wall in this region. These regional differences in mechanical behavior are consistent with previous findings in the literature, which have suggested that variations in hemodynamic forces and fiber orientation across the aorta may contribute to differences in mechanical performance.

In addition to the differences between layers and regions, the study also examined the relationship between mechanical properties and patient-specific factors, such as age, gender, and valve morphology. The results indicate that younger patients generally exhibited higher stress values in both the elastic and plastic regions of deformation compared to older patients. This finding aligns with established knowledge about the effects of aging on the aortic wall, including increased stiffness and reduced elasticity due to the accumulation of structural changes such as collagen cross-linking and elastin degradation. The presence of bicuspid aortic valve (BAV) also influenced mechanical behavior, with BAV patients displaying lower mechanical resistance, particularly in the outer layers, compared to patients with tricuspid aortic valve (TAV). This finding is consistent with studies such as those by Pasta et al., which have demonstrated that the altered hemodynamics associated with BAV contribute to earlier structural weakening of the aortic wall, leading to increased susceptibility to rupture.

One of the strengths of this study is its detailed analysis of the mechanical behavior of the aortic wall across different layers and regions, providing a nuanced understanding of how rupture propagates through the wall in aneurysmatic aortas. The finding that the inner layers are mechanically stronger than the outer layers is of particular clinical significance, as it suggests that interventions aimed at reinforcing the outer layers of the aorta may help prevent rupture in patients with aneurysms. Additionally, the regional differences in mechanical properties observed in this study highlight the importance of considering anatomical location when assessing rupture risk in patients with aortic disease. Regions such as the posterior and right lateral areas, which exhibited higher mechanical resistance, may be less prone to rupture, while the anterior and left lateral areas, which demonstrated lower mechanical strength, may require closer monitoring or earlier surgical intervention.

The study's broader relevance lies in its potential to enhance clinical management strategies for aortic aneurysms and dissections. By understanding the mechanical weaknesses in specific layers and regions, clinicians can more accurately identify patients at greater risk of rupture and tailor treatments accordingly. For instance, earlier surgical interventions could be prioritized for patients with aneurysms in weaker regions, while those with conditions like bicuspid aortic valve (BAV) may require intensified monitoring and management. The findings also underscore the importance of personalized treatment plans in aortic disease, factoring in patient-specific variables such as anatomical location, age, and valve structure, to improve clinical outcomes.

In conclusion, this study successfully achieved its objectives by providing a detailed characterization of the mechanical properties of the aneurysmatic ascending aorta under radial tensile stress. The findings highlight the critical role of the intima-media interface in maintaining the mechanical stability of the aortic wall, as well as the vulnerability of the media-adventitia interface to rupture initiation. The regional differences in mechanical performance observed in this study also underscore the importance of considering anatomical location when assessing rupture risk. By integrating these findings with existing literature on aortic mechanics, this study contributes valuable data to the field and provides a foundation for future research aimed at improving the diagnosis and treatment of aortic aneurysms and dissections. Further research that combines mechanical testing with histological and imaging techniques will be essential for gaining a more complete understanding of the factors that influence aortic wall failure, ultimately leading to better clinical outcomes for patients with aortic disease.

Abstract

This study investigates the mechanical properties of the aneurysmatic ascending aorta through radial tensile testing, focusing on the behavior of different anatomical regions and layers of the aortic wall. The primary aim is to examine how rupture propagates between the intima-media and media-adventitia layers, and to assess how these mechanical properties vary across four anatomical regions (anterior, right lateral, posterior, and left lateral) of the aorta. Specimens from twelve patients were subjected to direct tension tests, with force-displacement curves used to analyze key mechanical parameters, including maximum force (F_{max}), yield force (F_{yield}), strain, and elastic modulus.

The samples were collected from patients at Hygeia Hospital between September 2023 and February 2024. The experimental procedures were conducted at the Center of Clinical, Experimental Surgery & Translational Research at the Biomedical Research Foundation of the Academy of Athens (BRFAA). For the mechanical testing, a fully automated Vitrodyne V1000 Universal tensile testing machine was used, equipped with specially developed specimen grips to ensure precise and consistent measurements during the direct tension tests.

The results were contextualized within the framework of existing literature on the mechanical behavior of the aortic wall, particularly in relation to rupture initiation and propagation. The study found that the intima-media interface exhibits significantly higher mechanical resistance, with greater Fmax and elastic modulus values compared to the media-adventitia interface, indicating that the inner layers of the aorta are stronger and more resistant to rupture. In contrast, the outer layers showed greater variability and lower mechanical resistance, making them more prone to rupture initiation. These findings align with previous studies that have demonstrated the mechanical vulnerability of the media-adventitia interface in pathological conditions such as aortic dissections. Furthermore, regional differences were observed, with the posterior and right lateral regions exhibiting higher mechanical resistance compared to the anterior and left lateral regions, suggesting that the structural integrity of the aorta varies across different anatomical locations. Patient-specific factors such as age, gender, and valve morphology also influenced the mechanical behavior of the aortic wall. Younger patients exhibited higher mechanical strength, while patients with bicuspid aortic valves (BAV) showed lower resistance to rupture compared to those with tricuspid aortic valves (TAV). These findings emphasize the importance of considering individual patient characteristics when assessing rupture risk and planning treatment. In conclusion, this study provides valuable insights into the layer-specific and region-specific mechanical properties of the aneurysmatic ascending aorta, highlighting the critical role of the intima-media interface in maintaining aortic integrity. The findings have significant implications for the clinical management of aortic aneurysms and dissections, particularly in terms of identifying patients at higher risk of rupture and tailoring interventions accordingly. Future research should focus on integrating mechanical testing with histological analyses to further explore the structural factors that influence aortic wall failure.

Introduction

Thoracic Aortic Aneurysms

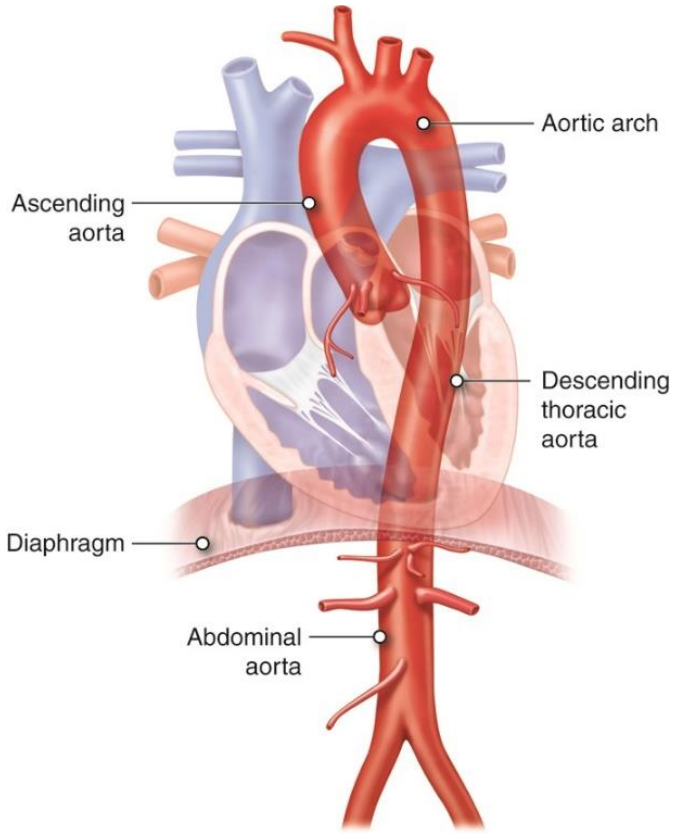

Figure 1: Parts of aorta in relation to heart and diaphragm. The ascending aorta, aortic arch, descending (thoracic) and abdominal aorta are shown. Retrieved from Anatomy & Physiology by Open Learning Initiative (CC BY-NC-SA). [1]

Definition

Thoracic aortic aneurysms (TAAs) are defined as localized dilations of the thoracic aorta that exceed 50% of its normal diameter. These aneurysms can develop in different regions of the thoracic aorta, such as the ascending aorta, aortic arch, or descending thoracic aorta, with some cases involving multiple sections. The majority of TAAs occur in the ascending aorta (60%), followed by the descending aorta (40%), and the aortic arch (10%) [2] [3].

An aortic aneurysm is a chronic condition involving the aorta and is marked by a permanent localized enlargement caused by adverse remodeling of the aortic wall. This disease can progress to a potentially fatal aortic rupture, which has a mortality rate exceeding 80%, leading to between 150,000 and 200,000 deaths annually worldwide [4], [5]. Aortic aneurysms are generally categorized as either thoracic (TAA), which occur above the diaphragm in the ascending aorta, aortic arch, or thoracic aorta, or abdominal (AAA), located below the diaphragm in the supra- or infrarenal regions [6]. Although the mechanisms differ between TAA and AAA, common risk factors include age, smoking, hypertension, hyperlipidemia, male gender, white race, and family history [7] [8]

Aortic aneurysms are characterized by gradual enlargement, which increases the risk of rupture and death [9]. Typically, thoracic aortic aneurysms remain clinically asymptomatic and progress slowly until reaching a critical size, after which the risk of aortic dissection or rupture rises. Contributing factors include bicuspid aortic valve, genetic syndromes like Marfan, Loeys-Dietz, and Ehlers-Danlos, as well as familial links. However, in many

instances, the cause is unknown. It is vital for clinicians to consider screening first-degree relatives of patients with aortic disease and to promptly refer patients to specialists in aortic conditions [10].

Prevalence

The detection rate of TAA has increased due to improved diagnostic techniques and greater awareness. While the commonly cited incidence is 10.4 per 100,000 patient-years, this figure likely underestimates the actual frequency of the disease. More accurate data come from studies combining hospital diagnostic records with autopsy findings. Olsson et al. [11] reported an incidence rate of 16.3 per 100,000 per year for men and 9.1 for women, while Clouse et al. [12] observed an incidence of 3.5 per 100,000 patient-years for both thoracic aortic dissection and rupture. In 2019, aortic aneurysms or dissections resulted in 9,904 deaths [13], but this figure is likely understated, as aortic dissection is often misdiagnosed as a myocardial infarction or other acute conditions in the absence of an autopsy.

TAAs are often called “silent killers” due to their asymptomatic nature but are linked to significant morbidity and mortality [14]. Approximately 22% of patients suffering from an acute aortic syndrome die before receiving medical care, and among those who do reach the hospital, 34% die within 30 days [11], [15]. Despite these alarming statistics, research into TAA remains limited compared to other cardiovascular diseases, emphasizing the need for deeper exploration of its pathophysiology to improve outcomes. While TAAs are more common in men, the prognosis is generally worse in women. Women with TAAs face a higher likelihood of aortic dissection or rupture, even at smaller aneurysm sizes, and they have higher mortality rates than men with the condition. These differences persist even when accounting for body size, implying that factors other than aneurysm size contribute to the worse outcomes in women. However, the reasons for this disparity remain insufficiently understood [16], [17].

Risk Factors, associations, and causes

Risk factors

Older age, Male sex, Hypertension, Smoking, Hypercholesterolemia, Weightlifting, Cocaine use, Trauma, Cardiovascular associations, Atherosclerosis, Other aneurysm, Prior aortic dissection, Aortic coarctation. [18]

Bicuspid aortic valve

Bicuspid aortic valve is the most common congenital anomaly affecting the aorta, found in 1% to 2% of the population. It is classified based on its anatomical appearance. Type 0 or true bicuspid valves lack a raphe and have two equally sized leaflets. More frequently, type I bicuspid valves possess a single raphe, generally between the right and left coronary cusps. Less commonly, the raphe forms between the right and noncoronary cusps. The raphe’s position can create specific flow patterns that may contribute to the formation of aortic aneurysms [19]. Patients with bicuspid valves are at increased risk for developing ascending aortic aneurysms, dissections, as well as aortic stenosis and regurgitation [20].

Genetic causes

Genetic causes of thoracic aortic aneurysms encompass several hereditary conditions, each with distinct pathophysiological mechanisms and risks for aortic disease.

Familial thoracic aortic aneurysm is a condition in which thoracic aortic aneurysms occur due to inherited genetic mutations. These mutations typically affect genes involved in the structure and function of the aortic wall. Familial cases tend to be inherited in an autosomal dominant pattern, meaning that a single copy of the altered gene from either parent can cause the condition. These individuals are at an increased risk of developing aneurysms or dissections at a younger age compared to sporadic cases, and close family members are often advised to undergo screening for aortic disease [21].

Marfan syndrome is an autosomal dominant disorder resulting from mutations in the FBN1 or FBN2 genes, which code for fibrillin-1 and fibrillin-2, respectively. These proteins are essential components of elastin-associated microfibrils, predominantly found in the tunica media of the aorta. Marfan syndrome is present in 4–5% of patients with aortic dissection. [22] The condition is characterized by the early development of aortic aneurysms

and dissections, along with skeletal features such as long limbs and fingers, and ocular problems like lens dislocation. Compared to non-Marfan patients, individuals with this syndrome experience aortic dissections at a significantly younger age (38.2 years versus 63.0 years) and tend to have fewer comorbidities like atherosclerosis and hypertension.

Loeys-Dietz syndrome (LDS) is an autosomal dominant disorder caused by mutations in the TGFBR1 and TGFBR2 genes, which are involved in the signaling pathways of transforming growth factor-beta. LDS shares similarities with Marfan syndrome, including a predisposition to aortic aneurysms and dissections. Almost 98% of LDS patients develop aortic root aneurysms, making them highly susceptible to aortic dissection. Patients with LDS often exhibit other systemic manifestations, including widespread arterial tortuosity, cleft palate, and skeletal malformations [23].

Ehlers-Danlos syndrome (EDS), particularly the vascular type (type IV), is an autosomal dominant disorder associated with mutations in the COL3A1 gene, which encodes type III procollagen. This type of collagen is critical for the structural integrity of blood vessels. Patients with vascular EDS are at a high risk of arterial rupture, which can occur even in the absence of aneurysms. In addition to arterial fragility, patients with vascular EDS may suffer from intestinal and uterine ruptures, making this the most severe form of EDS with the worst prognosis [24]. Vascular EDS is notable for its high morbidity and mortality, with many patients experiencing vascular events before the age of 40.

Turner syndrome, a chromosomal condition characterized by the absence of one X chromosome in phenotypic females (45X), is associated with several cardiovascular abnormalities, including bicuspid aortic valve, aortic coarctation, and aortic dilation. Patients with Turner syndrome are at an elevated risk for aortic dissection, particularly those with hypertension or structural heart disease. Over 90% of dissections in Turner syndrome patients involve these associated risk factors. Short stature and ovarian failure are common features, while cardiovascular anomalies significantly contribute to morbidity and mortality [25], [26].

Autosomal dominant polycystic kidney disease (ADPKD) is the most prevalent inherited cause of end-stage kidney disease, affecting hundreds of thousands of individuals worldwide. ADPKD is characterized by the development of fluid-filled cysts in the kidneys, leading to progressive renal dysfunction. In addition to renal manifestations, ADPKD is a multisystem disorder that can involve other organs, including the heart and vascular system [27]. Although the risk of aortic aneurysms and dissections in ADPKD remains unclear, there is evidence to suggest that these patients have an increased incidence of these complications compared to the general population. Cardiovascular complications are the leading cause of death in ADPKD patients, and studies have shown that their risk of aortic aneurysms and dissections is significantly higher than in the general population, [28].

Shprintzen-Goldberg syndrome (SGS) is a rare genetic condition characterized by craniosynostosis, which is the premature fusion of skull bones, leading to distinct craniofacial features. In addition to craniosynostosis, patients with SGS exhibit skeletal abnormalities such as scoliosis, joint hypermobility, and arachnodactyly. Cardiovascular manifestations of SGS include mitral valve prolapse, atrial septal defects, and aortic root dilation. Patients may also present with minimal subcutaneous fat, abdominal wall defects, and myopia [29]. Although SGS is a rare cause of aortic aneurysm, the presence of aortic root dilation increases the risk of aortic dissection in these patients.

Inflammatory causes

Takayasu arteritis is a chronic inflammatory disease that affects large arteries, including the aorta, causing vessel wall thickening, stenosis, and aneurysms. It predominantly affects young women and can lead to life-threatening complications if untreated [30].

Giant-cell arteritis is an inflammatory condition most commonly seen in older adults that affects large arteries like the aorta. It is associated with symptoms such as headache and vision problems, and it can cause aortic aneurysms due to inflammation and weakening of the arterial walls [31].

Behçet arteritis occurs in the context of Behçet's disease, a systemic vasculitis that affects both large and small vessels. It can lead to aneurysm formation in the aorta and other major arteries, particularly in populations from the Middle East and Asia [32].

Ankylosing spondylitis is primarily known for its effects on the spine, but it can also lead to aortitis, particularly involving the aortic root. This inflammation may cause aortic dilation and aneurysm formation, increasing the risk of serious complications [33].

Infective causes

Mycotic aortitis results from bacterial or fungal infections of the aortic wall, often secondary to conditions such as infective endocarditis. It weakens the aortic wall, potentially leading to aneurysm formation and rupture if not properly treated [34].

Syphilis, in its tertiary stage, can cause syphilitic aortitis, which affects the ascending aorta. This condition was a common cause of thoracic aortic aneurysms before antibiotics became widely available, leading to dilation and weakening of the aorta [35].

Idiopathic

In some cases, aortic aneurysms occur without a clearly identifiable cause. These idiopathic aneurysms are often discovered incidentally and still carry the risk of rupture or dissection, although the exact mechanisms behind their formation remain poorly understood [36].

Aortic Dissection

Definition

The etiology of an aortic aneurysm influences the likelihood of an aortic dissection. In advanced atherosclerosis, medial and adventitial fibrosis can inhibit the development of dissections [37]. Occasionally, atherosclerotic plaques may ulcerate, leading to limited dissections known as penetrating atherosclerotic ulcers, which are typically found in the descending thoracic aorta. Unlike aneurysms, these lesions show features such as intramural hematoma on imaging [38]. Conversely, conditions like Marfan syndrome, idiopathic thoracic aortic aneurysms (TAA), and TAA associated with bicuspid aortic valves frequently lead to dissections. This occurs because the medial degeneration seen in these conditions is marked by a lack of scarring, causing laminar weakness of the aortic wall. Some TAA cases with dissection lack an intimal tear, suggesting that the initiation of the dissection might involve ruptured or leaking vasa vasorum, which are more prominent in the proximal aorta [39]. Inflammatory aortitides like Takayasu arteritis often lead to aneurysms, but significant adventitial fibrosis prevents dissections despite medial inflammation. In contrast, giant-cell aortitis, with less fibrosis, is more often associated with aneurysms that lead to dissections.

Prevalence

Aortic dissection is a rare but highly fatal condition, making its overall incidence difficult to determine, as many patients succumb before diagnosis. Without treatment, the mortality rate of aortic dissection is around 40% at initial presentation, with the rate increasing by 1% per hour, potentially reaching an annual mortality rate of up to 90%. Population-based studies from Europe and North America between 1980 and 2015 reported an annual incidence of 2.5 to 15 per 100,000 [40].

Dissections or ruptures of ascending thoracic aortic aneurysms (aTAAs) are often lethal cardiovascular emergencies, with a 25% operative mortality rate despite advancements in surgery and intensive care, according to the International Registry of Acute Aortic Dissection (IRAD) [41]. While surgical repair decisions are based on factors such as size, growth, symptoms, family history, or connective tissue disorder, aortic diameter remains the primary criterion for risk stratification and surgical intervention. However, diameter alone is not always a reliable predictor. Studies show that nearly 60% of patients with Type A dissections had an aortic diameter under 5.5 cm,

and 40% had a diameter under 5.0 cm. This suggests that many dissections occur at smaller diameters, indicating a need for improved predictors of dissection risk in patients with diameters below 5.0 cm [42].

Assessment of Aortic Dimensions for Risk Stratification

Aortic Diameter

Guidelines currently recommend preventive open aortic repair when the aortic diameter reaches 55 mm. However, research has shown that this threshold may not be an ideal predictor of aortic events. A study based on serial imaging revealed that the mean ascending aorta size was 54.2 mm at the time of dissection, with an increase of 7.65 mm caused by the dissection itself. This study indicated that over 80% of ascending aorta dissections occurred at a diameter lower than 55 mm [43]. On the other hand, some studies support the 55 mm threshold, noting that it excludes 99% of patients from preventive surgery. Other researchers have proposed shifting the threshold to 50 mm in high-risk patients or those treated at specialized centers, where excellent surgical outcomes have been achieved [44]. Despite these findings, a study by Monaghan et al. supported current guidelines, showing similar survival outcomes between patients monitored with diameters of 50-55 mm and those who underwent immediate surgery once their diameter reached 55 mm. However, this study was limited by its small sample size and the presence of confounding variables [45].

Aortic Size Indexes

Research by Zafar et al. demonstrated that indexing aortic size to biometric data improves risk assessment for rupture, dissection, or death in patients with ascending thoracic aortic aneurysms. This method accounts for individual differences in body size, which can affect the interpretation of aortic dimensions. For example, smaller individuals with a high aortic-to-body-size ratio face greater risk and may require earlier surgery. The aortic size index, calculated by dividing aortic diameter by body surface area, correlates with the risk of aortic catastrophes, with an index of 4.25 cm/m² associated with a 20% annual risk of rupture or dissection. This index also relates to measures of aortic stiffness, such as systolic distension and diastolic recoil, which may provide further insights into disease severity [46], [47].

Aortic Length

Aortic length is an important factor in the natural history of ascending thoracic aortic aneurysms and is being explored as a predictive tool for better risk stratification. This measure, typically from the aortic annulus to the innominate artery, has been shown to predict aortic adverse events more effectively than diameter alone. Wu et al. introduced the aortic height index, which incorporates both length and diameter. This index outperforms diameter alone in predicting long-term outcomes [48]. Other studies have found that aortic volume and length assessments have superior diagnostic accuracy compared to maximum diameter measurements, and lowering the diameter threshold to 50 mm could significantly increase diagnostic sensitivity. Accurate measurement of aortic length also enables precise calculation of pulse wave velocity, an important factor in risk stratification [49].

Measurements of Aortic Dimensions

Magnetic resonance imaging (MRI) offers high-quality, reproducible measurements of aortic dimensions, including the aortic root, ascending aorta, and arch. MRI can also assess functional parameters such as aortic strain, distensibility, and pulse wave velocity, making it an excellent tool for monitoring treatment responses. Advanced MRI techniques, such as 4D flow MRI, further characterize altered aortic geometry and function, providing insight into the progression of aneurysm disease. Contrast-enhanced CT angiography also provides reliable aortic measurements, although it involves radiation exposure. Transthoracic echocardiography (TTE) is effective for measuring the aortic root but less so for the aortic arch, while transesophageal echocardiography (TEE) offers detailed imaging of the aortic root and ascending aorta, often used when MRI and CT are contraindicated [50].

Pathogenesis

Aortic dissection (AD) is fundamentally caused by an increase in pressure that separates the layers of the aortic media, creating a false lumen within the aortic wall. Two key factors drive this condition: the structural weakness of the aortic wall and increased wall tension. Several connective tissue components are implicated in AD pathogenesis, and genetic connective tissue disorders like Marfan and Ehlers-Danlos syndromes are significant predisposing factors. Damaged interlaminar elastic fibers lead to a weakened aortic media structure [51]. Additionally, fibrillin, a glycoprotein crucial for the organization of elastic fibers, contributes to this structural weakness, particularly in individuals with fibrillin-related disorders like Marfan syndrome. Furthermore, the degeneration of the aortic media is exacerbated by Medin, a fibril protein that forms oligomers and damages the aortic wall. Medin exerts its damaging effects via cytotoxicity to smooth muscle cells and by promoting matrix metalloproteinase (MMP) activity, accelerating the degradation of the extracellular matrix [52].

Hypertension, the most common condition associated with AD, emphasizes the role of wall tension. Elevated blood pressure increases mechanical stress on the aortic wall, which, over time, contributes to the weakening and dissection of the aorta. Interestingly, most hypertensive patients do not develop dissections, suggesting that degenerative changes, such as medial degeneration, are crucial for dissection development. Biomechanical factors also play a critical role. For instance, the motion of the aortic root during systole increases the longitudinal stress on the aortic wall, with the greatest stress coinciding with common sites of Type A dissection [53]. Additionally, patients with AD often have a thinner tunica media, further predisposing the aortic wall to dissection [54]. However, no single factor fully explains AD onset; it is the interaction between these multiple factors that determines the risk, highlighting the complexity of AD pathogenesis.

In addition to AD, other aortic pathologies such as intramural hematoma (IMH) and penetrating atherosclerotic ulcer (PAU) are closely related. IMH arises from the rupture of vasa vasorum, leading to the accumulation of blood within the media, typically without an intimal tear, though it may progress to full AD in some cases [55]. In contrast, PAU occurs when an atherosclerotic plaque ulcerates and penetrates the media, creating an ulcer within the aortic wall that may also evolve into an IMH or full dissection. Unlike classic AD, which commonly affects the ascending aorta, IMH and PAU predominantly affect the descending aorta [40].

AD usually begins with a tear in the aortic intima, exposing the medial layer to the pulsatile blood flow. This tear often occurs in areas of greatest shear stress, such as the right lateral wall of the ascending aorta or the proximal segment of the descending aorta. As the blood enters the medial layer, it causes separation of the wall layers, leading to the formation of a false lumen. The dissection can propagate, causing either rupture (with adventitial disruption) or re-entry into the true lumen via another intimal tear. In cases of re-entry, the patient may remain relatively stable if adequate perfusion is maintained, while rupture usually leads to rapid exsanguination and death. In some cases, the false lumen may end in a cul-de-sac, forming a blood clot. Early thrombosis of the false lumen may result in a smaller lumen compared to the true lumen, but if thrombosis occurs later, the false lumen may enlarge and compress the true lumen, compromising systemic perfusion. Dissections can also extend into the branches of the aorta, further increasing mortality risk, particularly if coronary arteries are involved [56].

Electron microscopy studies have revealed that, at the site of dissection, the extracellular matrix is sparse in the medial layer, with disrupted and fragmented elastic lamellae and thinning or absence of smooth muscle cell basement membranes. The intima, however, often shows no significant changes in AD [57]. At the molecular level, AD is associated with the remodeling of the aortic wall, driven by inflammation and extracellular matrix degradation. Macrophages infiltrate the tunica media, releasing MMPs and pro-inflammatory cytokines, which degrade collagen and elastin fibers. Increased production of MMP-1, MMP-9, and MMP-12 accelerates extracellular matrix degradation, a process also observed in aortic aneurysm and Marfan syndrome [58]. The imbalance between MMPs and their tissue inhibitors (TIMPs) promotes proteolytic activity, further weakening the aortic wall.

Another molecular process implicated in AD is VEGF-mediated neoangiogenesis. VEGF (vascular endothelial growth factor) promotes angiogenesis and has pro-inflammatory effects, contributing to the remodeling of the aortic wall. VEGF production is increased in the neo-vessels and immune-inflammatory infiltrates surrounding the degraded medial layer in AD. Hypertension exacerbates this process by acting as both a mechanical stressor

and a pro-inflammatory trigger. Hypertensive patients display elevated levels of pro-inflammatory molecules such as IL-6, VEGF, MCP-1, MMP-2, and MMP-9, which further promote extracellular matrix degradation and contribute to the pathogenesis of AD [59]. This demonstrates the pivotal role of inflammation and extracellular matrix degradation in AD development, particularly in hypertensive patients [60].

Classification

Aortic dissection is classified based on the anatomical location of the dissection. The Stanford classification system categorizes dissections into two types: Type A involves the ascending aorta or aortic arch, which is the section proximal to the left subclavian artery, whereas Type B dissections are limited to the descending thoracic aorta. [61] Furthermore, dissections are subdivided by their chronicity. Dissections presenting within 14 days of symptom onset are termed acute, while those that persist beyond two weeks are classified as chronic. Additionally, dissections may be described as complicated or uncomplicated. Complicated dissections involve conditions such as rupture or impending rupture, severe aortic valve insufficiency, coronary artery involvement, unmanageable hypertension, cardiac tamponade, neurological impairment, or intractable pain. When dissection affects branch vessels, it can result in either static or dynamic obstruction. Static obstruction occurs when the false lumen extends into the branch vessel, restricting flow in the true lumen. In dynamic obstruction, the dissection flap prolapses over the branch vessel, limiting blood flow without penetrating the branch itself. The classification of these obstructions is critical in determining the appropriate endovascular treatment options [62], [63].

Diagnosis

Aortic dissection typically presents with the sudden onset of severe chest or back pain, which patients often describe as “tearing” or “ripping.” This pain may migrate along the body depending on the location and extent of the dissection. Other diagnostic signs can include neurological deficits, signs of organ dysfunction due to compromised blood flow, differences in pulse strength between limbs, and a murmur caused by aortic valve insufficiency. [61] Diagnostic imaging is crucial for confirming the diagnosis, identifying the location and severity of the dissection, and guiding treatment decisions. Contrast-enhanced computed tomography angiography (CTA) is often the preferred imaging method due to its accessibility, rapidity, and non-invasive nature. CTA provides high-resolution images that can clearly display the dissection flap and determine the patency of both the true and false lumens. Other diagnostic techniques include echocardiography (transthoracic or transesophageal) and magnetic resonance angiography (MRA). In severe cases requiring immediate surgical intervention, invasive angiography may be employed for rapid diagnosis and preoperative planning [64].

Clinical Features

The clinical presentation of aortic dissection varies, largely depending on the location and extent of the dissection. The hallmark symptom is acute, severe pain, often described as tearing or stabbing, most commonly localized in the chest, back, or abdomen. Chest pain is present in approximately 80% of cases, though it is less common in Type B dissections, which may present with back or abdominal pain instead. Pain is often migratory, following the extent of the dissection [65]. Sensitivity and specificity studies indicate that acute chest pain is a highly predictive symptom of AD, with a sensitivity of 82.9% and specificity of 70.7% [66]. Other symptoms can include syncope, which occurs in around 15% of Type A dissections and often signals severe complications such as cardiac tamponade or aortic rupture, both associated with high mortality. Additional clinical features may include pulse deficits and signs of end-organ ischemia, although these are less common [40].

Prediction Methods

Biomechanically motivated models are often used to predict the rupture risk of aortic aneurysms and dissections, focusing on stress distribution and strength of the aortic wall. A key factor is that certain areas of the aorta, such as the region attached to the left pulmonary artery and the vertebral column, experience higher stress concentrations due to restricted movement, contributing to rupture risk. Additionally, variations in the aortic wall's composition, such as differences in collagen and elastin content, also play a role in determining the strength of the aortic wall in specific areas, leading to localized weakening. Models that integrate these biomechanical factors are used to assess the likelihood of rupture.

Inflation tests using silicone models of abdominal aortic aneurysms (AAA) demonstrated that ruptures tend to occur in regions of peak wall stress, rather than at the site of maximum diameter, a finding supported by computational models [67]. Similar results were found in normal thoracic aortas, where peak wall stresses were localized above the sinotubular junction and near the left subclavian artery, aligning with common sites of dissection initiation [68]. These findings emphasize that wall stress, rather than aortic diameter, is a more reliable predictor of rupture.

Models like the Probabilistic Rupture Risk Index (PRRI), which integrate both wall strength and stress distribution, further support this notion, showing strong correlations with arterial pressure but not with aneurysm diameter. This undermines the conventional reliance on diameter as a key rupture predictor [69]. Research also suggests that enzymatic activity may weaken specific regions of the aortic wall, thus increasing rupture risk, while statistical models incorporating wall stress and strength heterogeneity offer enhanced predictive value [70]. These principles have been incorporated into rupture risk calculation software, which focuses on external loads and geometry rather than patient-specific material parameters.

Additional studies have introduced alternative rupture risk criteria. A comparison of maximum diameter, rupture risk index, and overpressure index revealed weak correlations between diameter and the other two measures. Another rupture risk criterion based on maximum stretch parameters showed a strong association between tissue stretch and physiological elastic modulus, though this method has yet to see clinical application [71].

Further exploration of rupture risk, by examining ratios of systolic to rupture or yield diameters, found significant relationships with systolic blood pressure and wall tension, but not with aneurysm diameter. Finite element analyses reinforced the conclusion that rupture risk is more accurately predicted by peak wall stress and tension-strain modulus than by overall diameter, thus supporting the argument that biomechanical models provide superior rupture predictions compared to diameter-based approaches. [72].

Treatment

Currently, surgical repair remains the primary treatment option for aortic dissection to prevent aortic rupture, as no effective pharmaceutical therapies have been proven to halt the progression of aortic growth or prevent rupture. While surgical techniques have become more advanced and less invasive, there remains a strong need to explore alternative medical treatments targeting the underlying mechanisms of aneurysm formation and dissection [73].

Endovascular treatments like thoracic endovascular aortic repair (TEVAR) have largely replaced open aortic surgery for managing distal aortic dissections. However, for acute Type A aortic dissections, open surgery remains the gold standard. TEVAR has been applied in a limited number of Type A cases, mainly in patients deemed high-risk for surgery due to advanced age or comorbidities. The major challenge of using TEVAR in the ascending aorta is the dynamic motion of the aorta and the proximity to critical anatomical structures, such as the aortic valve, coronary arteries, and supra-aortic vessels. Endografts specifically designed for the ascending aorta are not yet widely available, limiting the current application of endovascular treatment in Type A dissections [74], [75].

Another innovative surgical technique, Personalised External Aortic Root Support (PEARS), involves placing a customized mesh sleeve around the aorta to halt its dilation and reduce dissection risk. Long-term follow-up of almost 400 cases has shown promising results, with PEARS effectively preventing further aortic root enlargement and dissection [76].

Preventing the dilation and rupture of the false lumen over the long term is another area of active research. One promising approach involves inducing complete thrombosis of the false lumen by occluding entry or re-entry tears. This can be achieved using stent-graft coverage or through endovascular techniques with vascular occluder devices and coils. Initial results from selected cases have demonstrated the feasibility and benefits of this approach in reducing the risk of rupture [77].

Follow-Up and Surveillance

Given that aortic dissection can affect the entire aorta and its branches, regular follow-up and long-term surveillance are essential for optimizing patient outcomes. Studies show a 10-year survival rate of 30–60% in patients with acute aortic dissection. Medical management, including the use of beta-blockers, angiotensin-II receptor blockers, and statins, is crucial to maintaining blood pressure control and reducing inflammation. Imaging studies, especially ECG-gated CTA or MRI, are key in monitoring patients for signs of disease progression or post-surgical complications. Patients with genetic predispositions for aortic dissection require even more careful monitoring and personalized care plans, which may include lifestyle modifications, family planning, and pre-emptive surgeries. Genetic counseling plays a vital role in managing these patients by assisting with pre-symptomatic genetic testing and family pedigree analysis [76].

Patients often face both physical and psychological challenges following treatment for aortic dissection. The traumatic nature of the condition, combined with the stress of long-term management, can result in significant emotional distress. Multidisciplinary care, including mental health support and patient-centered rehabilitation, is recommended to address these complex needs [78].

Mental Health Impact

Quality of life is significantly impacted in patients who experience aortic dissection (AD), particularly in terms of mental health and physical functioning. The diagnosis often triggers severe existential fears, as patients confront their mortality, with some expressing concerns about survival during hospitalization [79]. Even after discharge, patients remain hyper-aware of their physical condition, worrying about the possibility of recurrence or complications, which further contributes to stress. Compared to individuals who undergo surgery for chronic conditions like aortic valve replacement, AD patients exhibit lower quality of life (QoL), especially in areas such as vitality and mental health, partly because AD typically affects individuals who were otherwise healthy before the dissection. However, long-term improvements in health-related QoL (HRQoL) have been observed, with some studies showing better mental health outcomes over time, particularly as physical symptoms like pain subside and patients regain functionality [80].

Post-traumatic stress disorder (PTSD) is a common issue in patients with acute Type A aortic dissection, with about 23% of patients screening positive for PTSD, often experiencing persistent hypervigilance and reliving the traumatic event for several years after the dissection. Postoperative complications increase the likelihood of PTSD symptoms, while factors like regular exercise and employment appear to reduce its prevalence. Emergency surgery, especially in genetic conditions like Marfan syndrome, exacerbates patient anxiety, whereas minimally invasive procedures have been associated with better outcomes, regardless of whether the surgery was emergent or elective [81].

Post-traumatic growth (PTG), a phenomenon in which individuals experience positive psychological changes following trauma, has also been studied in cardiac patients, including those with aortic dissection. Factors such as personality traits, cognitive processing, and social support play critical roles in the likelihood of PTG, with extraversion being particularly associated with higher rates of growth. Insights from PTG in other cardiac conditions suggest that spiritual and faith-based factors may also contribute to positive long-term outcomes in aortic dissection patients [82].

Aortic Wall Structure

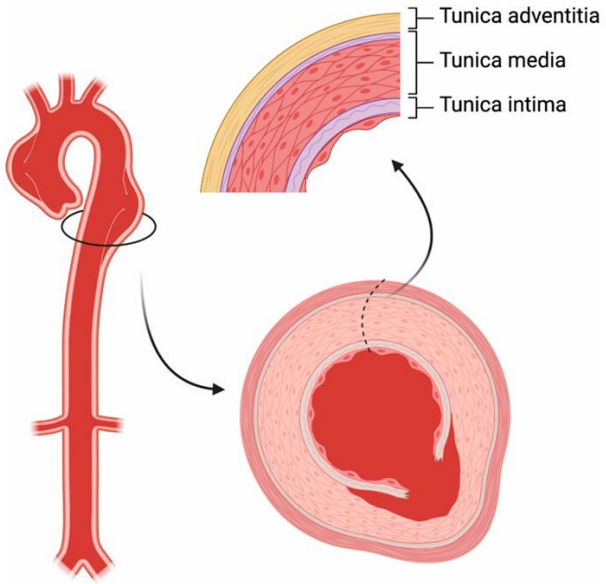

Figure 2: The structure of aortic wall. In aortic dissection, a tear in the intima allows blood to enter the media, forming an intimal flap and dividing the vessel into a true and false lumen. [76]

The aortic wall is composed of three layers, each with distinct structural and functional components: the tunica intima, tunica media, and tunica adventitia. Each layer contributes uniquely to the mechanical properties, resilience, and function of the aorta, and they undergo different changes throughout life due to aging, disease, and mechanical stress.

The **tunica intima** is the innermost layer of the aorta, and it plays a crucial role in maintaining the smooth interaction between blood flow and the vessel wall. This layer is primarily composed of endothelial cells, which form a monolayer that lines the lumen of the vessel. These endothelial cells are responsible for regulating vascular tone, maintaining a non-thrombogenic surface, and modulating inflammation. Endothelial cells release nitric oxide (NO), a vasodilator that helps maintain vessel relaxation and prevent platelet aggregation. This regulatory function of the intima is vital for preventing blood clot formation (thrombosis) and ensuring smooth blood flow. Beneath the endothelium, there is a thin layer of connective tissue known as the subendothelial layer, which includes elastic fibers. These fibers allow the aorta to stretch and recoil during the cardiac cycle. In young, healthy individuals, the intima is relatively thin, consisting primarily of the endothelial cells and the underlying internal elastic lamina, which separates the intima from the tunica media. However, with age, the intima thickens due to the accumulation of extracellular matrix proteins, mesenchymal cells, and lipids, leading to conditions such as atherosclerosis [83]. In this process, plaques form within the intima, narrowing the lumen and reducing blood flow. This thickening also contributes to the overall stiffening of the aorta, compromising its elastic properties and predisposing it to conditions like aortic dissection.

The **tunica media** is the thickest and most structurally significant layer of the aortic wall, responsible for its elastic and contractile properties. The media is composed of smooth muscle cells (SMCs), elastic fibers, collagen, and proteoglycans, organized into lamellar units. Each lamellar unit contains two elastic laminae, between which smooth muscle cells and connective tissue are arranged. These lamellae are critical for the elasticity of the aorta, allowing it to expand and recoil in response to pulsatile blood flow. The number of lamellar units in the tunica media increases with the diameter of the aorta. In the ascending aorta and aortic arch, there can be up to 60 lamellae in adults, while the descending aorta contains fewer lamellae, typically between 28 and 30 [84]. This regional variation reflects the different embryological origins of smooth muscle cells within the aorta. The SMCs in the ascending aorta and arch originate from the neural crest (ectoderm), while those in the descending aorta

are derived from the paraxial mesoderm (somites). Despite these differences, the ratio of aortic diameter to medial thickness remains consistent throughout the aorta, which ensures that the mechanical load is evenly distributed. The elastic fibers in the tunica media are essential for the aorta's ability to absorb the energy of each heartbeat and maintain continuous blood flow during diastole. As the aorta expands under pressure, these fibers stretch and store mechanical energy, which is then released as the vessel recoils. This elastic property is crucial for reducing the workload on the heart and maintaining steady blood flow throughout the arterial system. Collagen fibers in the media provide additional tensile strength, preventing overstretching of the aorta, while proteoglycans help bind water and regulate tissue resilience. With aging, the tunica media undergoes significant changes, including medial degeneration (MD) [85]. MD is characterized by the breakdown of elastic fibers, increased collagen deposition, and loss of smooth muscle cells. These changes lead to reduced elasticity and increased stiffness, which compromise the aorta's ability to withstand pulsatile stress. In conditions such as aortic aneurysms or Marfan syndrome, the media is particularly affected, as defects in the connective tissue can lead to progressive weakening and dilation of the aorta, increasing the risk of rupture.

The **tunica adventitia** is the outermost layer of the aortic wall and provides structural support and protection. It is composed of loose connective tissue, primarily collagen fibers, fibroblasts, and elastin. The adventitia contains the vasa vasorum, a network of small blood vessels that supply the outer part of the aortic wall, particularly the tunica media and adventitia, with oxygen and nutrients [86]. This is crucial for the survival of the outer layers of the aorta, as diffusion from the lumen alone is insufficient to nourish the thick walls of large vessels like the aorta. The adventitia also contains nerve fibers from the autonomic nervous system, which help regulate vascular tone by controlling the contraction and relaxation of smooth muscle cells in the media. This layer is critical for the mechanical integrity of the aorta, as the collagen fibers within the adventitia provide tensile strength that prevents overexpansion and rupture under high-pressure conditions. As the aorta ages, the adventitia becomes thicker due to increased collagen deposition, contributing to overall vessel stiffness. The presence of inflammatory cells in the adventitia, particularly in pathological conditions like aortic aneurysms, can accelerate degeneration of the medial layer, further weakening the aortic wall. In aortic dissections, the integrity of the adventitia is particularly important, as rupture or weakening of this layer can lead to catastrophic outcomes, such as full-thickness rupture of the aortic wall. [87]

Biomechanics of aorta

The aorta behaves like an inflated tube, where arterial pressure creates mechanical stress, particularly circumferential and axial stress, which are the main forces acting on the aortic wall. As the aorta expands, its tissue volume stays constant, causing wall thinning due to stretching in both the circumferential and axial directions. In larger aortas, the wall becomes thicker due to an increase in medial lamellar units (MLUs), which maintain a consistent tension per MLU at approximately 2.0 ± 0.4 N/m [88]. Under normal arterial pressure, the circumferential wall stress in the ascending aorta measures around 92.51 ± 6.35 kPa [89]. Given that the aorta experiences dynamic pressure fluctuations with the cardiac cycle, the stress and strain within the wall oscillate accordingly. Additionally, the aorta becomes stiffer under hypertensive conditions compared to normal pressure levels, as stiffness increases with strain. Like other vessels, the aorta exhibits anisotropy, displaying different stiffness characteristics along the circumferential and longitudinal axes.

Regarding wall shear stress (WSS) and strain due to blood flow, the aortic blood flow is unsteady, posing challenges to assumptions based on Poiseuille flow. Although the majority of blood flow occurs in the downward direction during most of the cardiac cycle, it reverses in late diastole. While a non-Newtonian model may be necessary to capture specific local blood flow characteristics, a Newtonian fluid model is sufficient for predicting WSS in large arteries like the aorta [90]. Haemodynamic factors, such as WSS, play a pivotal role in the development of vascular diseases, including aneurysms and atherosclerosis. Flow patterns impact disease progression by affecting endothelial homeostasis and influencing the behavior of smooth muscle cells and fibroblasts [91].

Flow patterns within the thoracic aorta vary depending on valve morphology. In healthy individuals with tricuspid aortic valve (TAV), blood flow is broad and centrally distributed, whereas BAV patients exhibit asymmetric, high-velocity jets near the aortic wall. The flow angle is also elevated in BAV, which contributes to increased regional

WSS in the ascending aorta [92]. Velocity streamlines in TAV show laminar flow parallel to the aortic wall, while BAV cases display eccentric jets that disrupt the flow and impinge on the greater curvature. Helical flow, which involves significant radial components, is another important aspect of thoracic aortic dynamics. This flow pattern results from factors such as ventricular twist, the mechanics of the aortic valve and root, and the curved morphology of the aorta [93]. Although helical flow can support normal organ perfusion, it is also implicated in plaque deposition. Differences in monocyte adhesion to the vascular wall, a critical factor in plaque formation, are linked to the radial component of velocity. In BAV patients, abnormal right-handed helical flow is associated with increased rotational flow, elevated WSS, and larger ascending aortas, particularly in cases of right-non cusp fusion [94]. However, some BAV patients with normal flow patterns exhibit WSS and aortic dimensions similar to those of healthy individuals.

Literature Review

In recent years, the study of the mechanical properties of the aortic wall, particularly through direct tension testing in the radial direction, has been instrumental in understanding the underlying mechanisms that contribute to aortic dissection, aneurysm formation, and eventual failure. Aortic dissection, a serious and often fatal condition, involves the tearing of the aortic wall layers, typically propagating between the media and adventitia. This mechanical failure highlights the significance of understanding the tensile properties of the aortic wall in the radial direction, as these properties offer insight into how the wall withstands mechanical stress and the factors that lead to its failure.

Radial tensile testing, as used by Sommer et al., provides a direct method to evaluate the strength of interlamellar connections within the media, a critical factor in dissection propagation. Their study revealed that radial failure stress in human abdominal aortas averaged 140.1 ± 15.9 kPa, a significant value that demonstrates the mechanical resilience of the aorta in the radial direction, though it was still lower compared to the circumferential and longitudinal directions [95]. This lower radial stiffness, compared to other directions, reflects the anisotropic nature of the aortic wall, which is structured to handle mechanical stress more effectively in the circumferential direction, where blood pressure exerts the greatest force. The findings of MacLean et al. support this, with their comparison of porcine thoracic aortas showing that radial failure stress was approximately half of that in the longitudinal and circumferential directions (61.4 ± 4.3 kPa versus 112.7 ± 9.2 kPa and 151.1 ± 8.6 kPa, respectively) [96]

This discrepancy between the radial and circumferential mechanical properties underscores the role of the aortic wall's layered structure. The aortic media, composed primarily of elastin and collagen, contributes to the wall's elasticity and strength. However, the behavior of these fibers differs depending on the direction of applied stress. In the circumferential direction, collagen fibers align and stiffen in response to increased strain, contributing to the wall's ability to resist higher forces. In the radial direction, however, the fibers are less aligned and provide less mechanical support, which is reflected in the lower failure stress values observed in radial tensile tests [97]. This difference in fiber alignment and behavior is critical to understanding why the aortic wall tends to fail through peeling mechanisms, as observed in radial dissection studies. As the wall separates between layers, the elastin fibers lose cohesion, leading to lamellar decohesion, a process documented in several studies [98]

Further supporting these findings is the work of Schriefl et al., who analyzed the ultimate tensile stress in the radial, circumferential, and longitudinal directions. Their results indicated that the mechanical strength in the circumferential direction (1282 ± 822 kPa) far exceeded that in the radial direction (131 ± 56 kPa) [99]. This anisotropic behavior can be explained by the preferred alignment of collagen fibers in the circumferential direction, which allows the aortic wall to withstand higher pressures from blood flow while sacrificing strength in the radial direction. Such anisotropy is crucial for the aorta's function, as it needs to remain elastic enough to accommodate pulsatile blood flow, while still resisting circumferential expansion. [100]

A critical aspect of understanding the mechanical behavior of the aortic wall is recognizing the differences in mechanical properties across individuals, particularly in patients with aortic pathologies. Pasta et al. [101] studied the mechanical properties of aortic tissue in patients with ascending thoracic aortic aneurysms (TAA), comparing the delamination strength of the intima and adventitia in individuals with bicuspid aortic valves (BAV) and tricuspid aortic valves (TAV). Their results indicated that the intimal portion of the aortic wall failed before the adventitial portion in patients with TAA, with the delamination strength significantly lower in those with BAV compared to TAV patients. This finding highlights the impact of valve morphology on the mechanical properties of the aortic wall, as the altered hemodynamics in BAV patients may lead to earlier or more severe structural weakening. The importance of considering anatomical variations, such as valve morphology, is thus critical for understanding patient-specific risks of aortic dissection and aneurysm formation.

The structural integrity of the aortic wall, particularly in the context of radial tension, has also been explored through direct tension testing on healthy and pathological tissues. Sommer et al. [102] observed that during radial tension tests, the aortic media exhibits a linear elastic response at small displacements, followed by a region of damage accumulation and eventual tissue failure. This behavior reflects the inherent limitations of the

radial direction in handling stress, with the aortic media showing limited elasticity compared to the circumferential direction, where collagen fibers progressively recruit to provide increasing stiffness [103]. The average radial stiffness values reported in this study (559 ± 264 kPa) align closely with circumferential stiffness values in the literature, reinforcing the idea that while the aortic wall is anisotropic, it still exhibits considerable mechanical resilience across different directions of stress [104].

Direct tension testing has also been instrumental in revealing the failure mechanisms of diseased aortic tissue. In their study on atherosclerotic intima-media specimens, researchers observed that these tissues exhibited significantly lower radial failure stresses compared to healthy tissues [105]. The presence of atherosclerotic plaques, associated with intimal thickening and calcification, contributes to the stiffening of the arterial wall, reducing its ability to deform elastically. The resulting mechanical response is characterized by a steep initial slope in the force-displacement curve, followed by a nonlinear region where tissue defects begin to form. Ultimately, the tissue fails at much lower stresses than healthy specimens, reflecting the impact of disease on the mechanical integrity of the aortic wall.

The anisotropy of the aortic wall, with its lower mechanical strength in the radial direction compared to the circumferential direction, raises important questions about the mechanisms of dissection propagation. As shown in studies like those by Sommer et al. [98] and MacLean et al. [106], the peeling-like mechanism observed during radial failure likely stems from the lamellar structure of the media, where the separation of layers occurs more easily in the radial direction due to the weaker interlamellar bonds. This lamellar separation is particularly relevant in the context of aortic dissections, where the dissection often propagates tangentially, either circumferentially or longitudinally, once initiated. The low radial failure stress suggests that once a tear occurs in the aortic wall, it can easily spread along the lamellae, contributing to the rapid progression of aortic dissections.

These findings have significant implications for the clinical understanding of aortic dissection and aneurysm formation. Understanding the directional differences in mechanical properties is essential for assessing the risks associated with aortic wall failure, particularly in patients with predisposing conditions like BAV, TAA, or atherosclerosis. The lower delamination strength in BAV patients, as highlighted by Pasta et al., suggests that such individuals may be at higher risk for early dissection or aneurysm rupture [101]. These insights underscore the importance of personalized approaches in the diagnosis and management of aortic disease, where valve morphology, age, and the presence of atherosclerotic disease must all be considered when assessing a patient's risk profile.

Additionally, future studies would benefit from incorporating microscopic histological analyses alongside mechanical testing, as this would provide a more detailed understanding of the underlying structural changes that contribute to the observed mechanical behaviors. Histological studies could reveal how the distribution of collagen and elastin fibers, as well as the presence of microdefects, affects the mechanical response of the aortic wall under radial tension. Such analyses would be particularly valuable in understanding the progression of diseases like atherosclerosis and aneurysms, where tissue degeneration plays a key role in weakening the wall and increasing the risk of failure [107].

Overall, the literature on radial tensile testing of the aortic wall highlights the importance of understanding the mechanical properties of the aorta in various directions, particularly in the radial direction where the wall is most vulnerable to failure. The anisotropic nature of the aortic wall, the role of valve morphology, and the impact of disease all contribute to the complex mechanical behavior of the aorta. These factors must be considered when assessing the risk of aortic dissection or aneurysm rupture, as they provide critical insights into the wall's ability to withstand mechanical stress and the factors that lead to its failure. As research continues, combining mechanical testing with histological analysis will provide a more complete picture of the factors driving aortic wall failure, ultimately contributing to better diagnostic and therapeutic strategies for patients with aortic disease.

Methodology

Material

In the present study, 12 human ascending aortas age range 33– 76 yr (mean 53,55 yr), ten males and two females were harvested during open surgical repair of ascending aortic aneurysms. After harvesting, the specimens were stored in a calcium-free and glucose-free 0.9% physiological saline solution at 4 °C until use. Use of material from human subjects was approved by the Ethics and Professional Conduct Committee of Hygeia. All tests were performed within 48 h from surgery. The period needed to collect the data is approximately six months, from September 2023 to February 2024. The following table presents in detail the age and gender of each patient.

#	Gender	Age	Valve Type	Hypertension	Aortic Valve Diseases	Other Syndromes
1	F	67	TAV	Yes	Regurgitation	No
2	M	50	TAV	Yes	No	No
3	M	54	TAV	Yes	Regurgitation	No
4	M	34	BAV	Yes	Regurgitation	No
5	M	33	TAV	No	Regurgitation	Marfan
6	M	74	TAV	Yes	No	No
7	M	76	BAV	No	Regurgitation	No
8	M	37	TAV	No	Regurgitation	No
9	F	56	TAV	No	Regurgitation	No
10	M	53	TAV	No	No	No
11	M	55	BAV	No	No	No
12	M	54	TAV	No	No	No

Table 1: Pre-operative patient characteristics.

Specimen Preparation

We conducted a mechanical failure test of the aortic wall layers of the specimens—direct tension test. Initially, the sections of thoracic aorta taken are examined for the presence of any loose adherent tissue or epicardial stroma and carefully cleaned. They are then cut in such a way that only the part of the ascending aorta of interest remains.

The AAos were then cut along the axial direction to obtain flat rectangular tissue sheets, as shown in the figures below. After converting the specimen into a longitudinal segment, its four regions are marked: the left and right lateral, the anterior and the posterior depending on its position in the aorta, as shown in Figure 4.

A B

Figure 3: (a) the part of the ascending aorta of interest. (b) The AAos were then cut along the axial direction to obtain flat rectangular tissue sheets

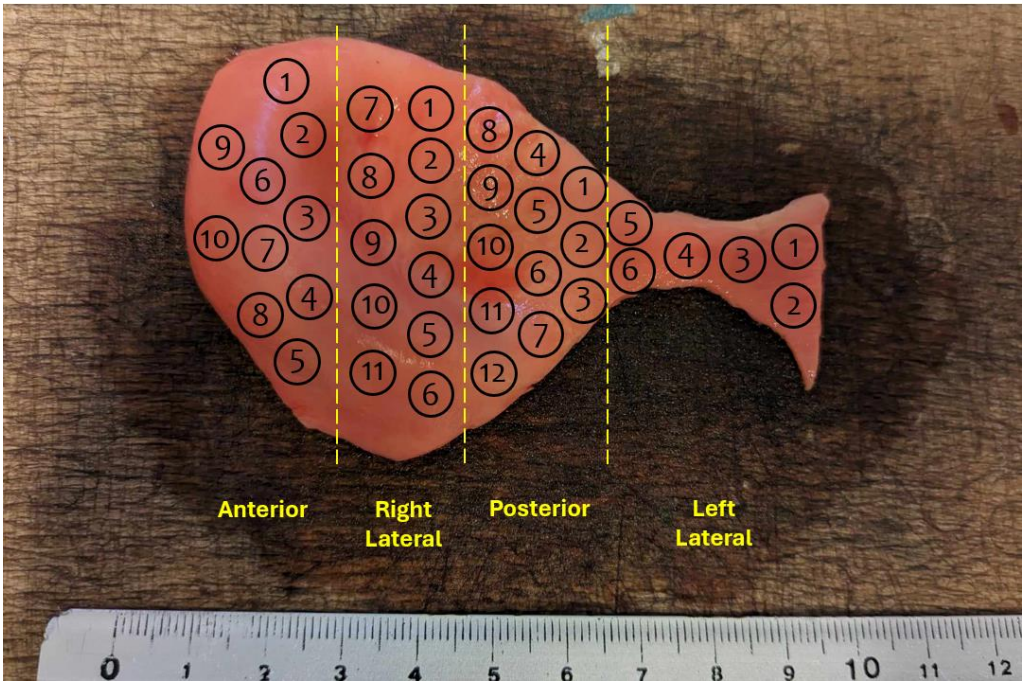

Figure 4: Patient11, After converting the specimen into a longitudinal segment, its four regions are marked: the left and right lateral, the anterior and the posterior depending on its position in the aorta. The exact location of each specimen is mapped, and a sketch is drawn representing each aortic sample divided into its individual segments.

A cylindrical blanking tool was used to punch out coin-shaped specimens from each region for the direct tension test (8.13±0.20 mm diameter, and 2.25±0.20 mm thickness). Radial tension test specimens were obtained from each of the 12 different ascending aortas (AAs). Multiple specimens were extracted from the same aorta. As shown in Fig. 4, coin-shaped specimens were taken from each quadrant of the ascending aortic wall. Depending on the size of the tissue and each section, a varying number of experiments were conducted for each case, with the left lateral quadrant yielding the fewest samples per patient due to its morphology.

The exact location of each specimen is mapped and a sketch is drawn representing each aortic sample divided into its individual segments. Above is an example of specimen mapping after processing the image of the aortic segment of patient 11.

Because the sample size examined was large, the need arose to apply some coding to facilitate the processing and recording of the results. Thus, each trial has a specific name, which is of the form: abcd where a, b, c and d are variables. The meaning of each variable is given below.

a: is used to denote the serial number of the patient. Each patient was assigned a number which indicates the order in which he/she was experimentally tested.
b: indicates the region in which the sample is located and can take the values: a for anterior, p for posterior, ll for left lateral and rl for right lateral.
c: shall be used to indicate the serial number of the specimen for that region. This number indicates the order in which it was experimentally tested.
d: can take the values in and out, and are used to indicate which layer the initial incision was made in, in for between intima and media and out for between media and adventitia.

Therefore, according to the above, the name for example 1ll2in, corresponds to a tissue that comes from the first patient tested, belongs anatomically to the left lateral region, is the second specimen in a row tested from this region and has an initial incision made between intima and media layer.

Prior to conducting the direct tension tests, final specimen preparations were essential. Just before mounting the specimens on the testing equipment, a precise circumferential incision was made around each coin-shaped specimen. This cut, approximately 1.0 mm in depth, resulted to reduced tissue diameter from its original 8.0 mm to a final 6.0 mm. The purpose of this undercut was to create a predefined site for failure initiation and it was carefully executed using a specially modified surgical blade. A superadhesive gel was used to ensure that the specimens remained firmly attached to the grips of the testing machine throughout the loading process. A visual representation of a specimen prepared for direct tension testing can be found in Figure 6.

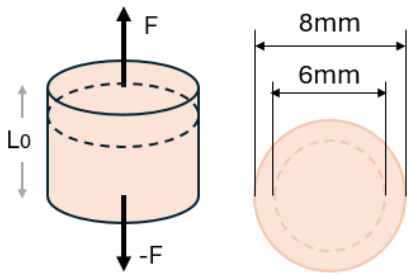

Figure 5: Schematic representation of the uniaxial tensile test. The applied tensile force is defined as F, the initial length of the specimen is L_0, and the elongation of the specimen is ΔL. Essentially, the experiment records the magnitude of ΔL as a function of the load (F).

Figure 6: A representative specimen, ready for a direct tension test

The process of making the initial incision into the arterial layers was carried out with meticulous surgical techniques, utilizing a fine scalpel. Two specific types of incisions were tested: for the **inner incision**, the dissection began between the intima and media layers of the arterial wall, while the **outer incision** initiated separation between the media and adventitia layers. These distinct regions were selected due to their differing mechanical properties, which allowed for a clear distinction between tissue behaviors during the separation process. The varying elasticity and structural composition of the layers made it possible to study the different mechanical responses of each.

Throughout the dissection and testing, every effort was made to minimize any unintended mechanical damage to the tissue layers. To ensure the integrity of the specimens, they were regularly immersed in a 0.9% physiological saline solution, which helped maintain their hydration and closely simulated in vivo conditions. Proper hydration was critical to preserving the tissue's natural mechanical properties and avoiding the degradation that could occur in a dry environment. This careful preparation and handling allowed for accurate and reproducible results, ensuring that the mechanical behavior observed during testing reflected the true characteristics of the tissues under investigation.

Mechanical Testing

Device

The mechanical properties of the aortic specimens were measured on a fully automated Vitrodyne V1000 Universal tensile testing machine (Liveco Inc, Burlington, VT, USA). This device has been specifically selected for performing uniaxial tensile testing experiments on biological tissues. The experiments were conducted at Biomedical Research Foundation (BRFAA) of the Academy of Athens, usually within 48 hours from surgery.

The tensile machine consists of the main tensile unit and the control unit. The tensile unit consists of the support base, two especially developed specimen grips, the drive piston and the load and displacement gauge, experimental setup shown in Fig. 7. The device is connected to a computer and by using appropriate software (Material Witness V2.0.2 Liveco Inc, Burlington, VT, USA) it is possible to store the load and displacement data (ForcePosition) for further processing.

The device for recording the intensive state is equipped with a force cell with a maximum load of 500g and a sensitivity of 0.25g and a maximum displacement of 20000um. No specimen showed tensile load resistance greater than 500g. The sampling frequency of the machine is set at 10Hz, i.e. one measurement is taken every 0,1sec. Of the two grips carried by the machine, the lower grip remains fixed, while the upper one is connected to the piston which exerts a tensile load on the specimens at a speed of 200 um/sec.

Figure 7: Experimental setup, the tensile machine consists of the main tensile unit and the control unit.

Direct Tension Test Protocol

Cyanoacrylate adhesive was applied to both the upper and lower grips of the testing apparatus. The coin-shaped specimen was carefully positioned onto the lower, stationary grip, after which a compression load of 1.0 N was exerted for approximately five minutes. This allowed sufficient time for the adhesive to fully react and bond the specimen securely. Before commencing the actual test, the specimen was thoroughly moistened with a 0.9% saline solution to maintain its physiological properties and prevent dehydration, ensuring that the test conditions closely mimicked a natural environment.

During the mechanical testing, the extension rate was precisely controlled at 1.0 mm/min, with continuous monitoring of the resisting force exerted by the specimen. This steady rate of extension ensured that the mechanical response of the material could be measured accurately throughout the test. The recorded force-displacement data provided insight into the specimen's behavior under tensile stress.

After the specimen had completely separated, the zero-load reference point was defined, marking the end of the test. Following this, the failure surface was inspected visually to identify the exact location of material failure. It was observed that, in several instances, the failure did not occur at the incision site but rather at the point where the specimen was attached to the grip using the adhesive. This type of failure, occurring at the bonded region, indicated that the specimen may not have been properly loaded or that the adhesive bond was weaker than the specimen's intrinsic material strength. As such, any tests where this form of adhesive failure was observed were discarded, and the data were not included in subsequent analyses.

For successful tests, where failure occurred at the intended location within the specimen, the results were considered valid. A representative image illustrating the final stage of a properly executed direct tension test is presented in Figure 8, showing the specimen at the moment of separation under tensile load. This visual confirmation served to validate the integrity of the test process and the accuracy of the data collected from specimens that failed at the expected region.

Figure 8: A representative photograph of the end stage of a successful direct tension test.

Analysis

Strength of materials

The aim of the current study is to calculate the mechanical properties of the layers of the thoracic aortic wall. In the failure analysis conducted, the following quantities are calculated: the stress of the tissue, the strain at this stress, and the modulus of elasticity, in elastic and plastic region and at the ending point each experiment.

Strength of materials is a fundamental concept in mechanics, focusing on the behavior of solid objects when subjected to external forces or loads. Understanding how materials respond to these forces—whether through deformation, stretching, or even failure—is critical in designing structures, devices, or biological systems that can withstand applied stresses. The study of material strength involves key parameters such as stress, strain, elasticity, plasticity, and failure mechanisms, all of which are essential for predicting how a material will behave under various conditions. These principles are particularly important when dealing with soft tissues, which exhibit complex mechanical behavior due to their viscoelastic and anisotropic nature.

To understand the strength of materials, it is necessary to first define **stress** and **strain**. Stress is a measure of the internal forces acting within a material in response to an applied load, and it is defined as force per unit area. Mathematically, stress is given by the equation:

$$\sigma = \frac{F}{A} \quad (N/m^2)$$

where σ represents stress, F is the applied force, and A is the cross-sectional area over which the force is distributed. Stress has units of pressure (typically Pascals in the SI system), and it provides insight into how much force is being applied to a material relative to its size.

Strain, on the other hand, is a dimensionless quantity that measures the deformation of a material in response to an applied stress. It is the ratio of the change in length to the original length of the material, defined by the equation:

$$\varepsilon = \frac{\Delta L}{L_0}$$

where ϵ is the strain, ΔL is the change in length, and L_0 is the original length of the material. Strain describes how much a material stretches or compresses when subjected to stress, and it is typically expressed as a percentage or a ratio.

The relationship between stress and strain can be represented by a **stress-strain curve**, which is a critical tool in the analysis of material strength. This curve provides a visual representation of how a material responds to increasing stress, showing the different regions of material behavior, from elastic deformation to plastic deformation, and finally, to failure.

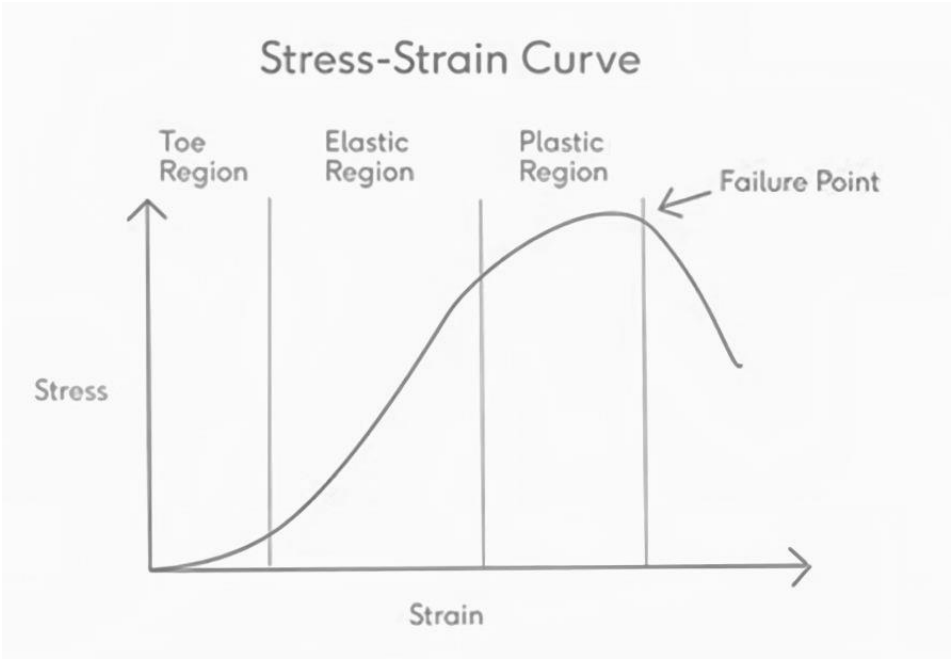

Figure 9: Typical stress-strain curve for soft tissue [108]

In the initial phase of the stress-strain curve, the material behaves elastically. In this **elastic region**, the relationship between stress and strain is linear, meaning that the material deforms proportionally to the applied load and returns to its original shape when the load is removed. This behavior is described by **Hooke's Law**, which states:

$$\sigma = E\epsilon$$

where E is the **Young's modulus** or **elastic modulus**, a constant that characterizes the stiffness of the material. For soft tissues, the elastic modulus is typically lower than that of rigid materials like metals or ceramics, reflecting their ability to deform more easily under stress. Soft tissues like skin, arteries, or tendons exhibit significant elastic behavior under physiological conditions, allowing them to stretch and recoil as needed without permanent deformation.

As the applied stress increases beyond the elastic limit, the material enters the **plastic region**. In this phase, the stress-strain relationship becomes nonlinear, and the material begins to deform permanently. This means that once the load is removed, the material will not return to its original shape. The onset of plastic deformation is marked by the yield point, which separates the elastic and plastic regions. For soft tissues, this plastic behavior may occur when subjected to abnormally high stresses, such as during trauma or pathological conditions, where permanent tissue damage can occur.

In the plastic region, the material exhibits strain hardening, meaning that additional stress is required to continue deforming the material. The curve continues to rise, but at a slower rate than in the elastic region. Eventually, the stress reaches a maximum value, known as the ultimate tensile strength (UTS). This point represents the highest stress that the material can withstand before it begins to fail.

Following the UTS, the material enters the necking region, where localized reduction in cross-sectional area occurs. As the material continues to deform, the stress begins to decrease, and the material approaches its fracture point, where it ultimately breaks apart. For soft tissues, the fracture point might correspond to a tear or rupture, such as the tearing of a ligament or the dissection of an artery. In such cases, the tissue has been overstretched beyond its physiological limit, leading to irreversible failure.

Processing Of Experimental Data

The goal of the present study is to investigate the dissection properties of the thoracic ascending aorta by means of direct tension tests. The direct tension test demonstrates the strength in the radial direction.

In this study, each specimen underwent a direct tension test, during which force and displacement were recorded continuously. This testing method allowed us to observe the mechanical behavior of the material until it ultimately failed. From the data obtained, we focused on key points along the force-displacement curves, such as the elastic region, the failure point, and the ending point, to further analyze the material's properties. For each test, we calculated stress, strain, and the elastic modulus, which were essential in understanding the behavior of the material under tension.

The force-displacement data collected from each test was used to generate a diagram for each specimen, which visually represented the material's response to the applied force. Initially, as the force increased, the material entered the elastic region, where displacement occurred proportionally to the applied force. This elastic behavior was characterized by a linear relationship between force and displacement, indicating that the material could return to its original shape after the load was removed. Identifying this region was crucial for calculating the elastic modulus, which reflects the stiffness of the material.

To determine the elastic modulus, we examined the slope of the force-displacement curve in this initial linear phase. A steeper slope in the elastic region indicated a higher elastic modulus, meaning the material exhibited greater resistance to deformation under applied stress. By calculating this modulus for each specimen, we obtained a measure of the material's inherent stiffness, which provided insight into its capacity to withstand mechanical loads. The elasticity of the material was thus a central parameter in understanding its mechanical properties, particularly its ability to maintain structural integrity under physiological conditions.

As the force continued to increase, the material began to exhibit plastic deformation. Beyond the elastic region, the force-displacement curve became non-linear, signifying that the material was undergoing permanent deformation. The plastic region was an important part of the analysis because it highlighted the material's ability to absorb energy and deform before reaching its failure point. The failure point was identified as the maximum value on the force-displacement curve. At this point, the material could no longer sustain the applied load, and its structural integrity was compromised. A sharp drop in force followed this point, marking the point of rupture of the specimen. After the failure point, the force rapidly decreased as the material was torn apart, and the curve approached the ending point. This point corresponded to the complete rupture of the specimen, and the force recorded at this stage was zero.

In order to perform a more detailed analysis, the force and displacement data were used to calculate the stress and strain at each of these key points. These values allowed us to translate the raw force-displacement data into more fundamental mechanical properties, providing a clearer understanding of the material's behavior independent of its specific geometry or size. The calculation of stress involved dividing the recorded force by the cross-sectional area of the coin-shaped specimen. This conversion allowed us to assess the intensity of the applied load relative to the size of the material, ensuring that the results were comparable across different patients and quadrants of aortic tissue. Strain, on the other hand, was calculated by dividing the displacement by the original length of the specimen, that here corresponds to the thickness of each specimen.

Once stress and strain were calculated, we generated stress-strain curves for each specimen. These curves offered a more precise representation of the material’s mechanical properties, as they eliminated the influence of specimen size and focused solely on the material's response to the applied load. The slope of the stress-strain curve in the elastic region was used to verify the elastic modulus calculated earlier from the force-displacement data, ensuring consistency across different analytical approaches.

For the analysis of the plastic region, a fourth-degree polynomial fitting was applied to the non-linear portion of the force-displacement curve.

$$\sigma(\epsilon) = a_4\epsilon^4 + a_3\epsilon^3 + a_2\epsilon^2 + a_1\epsilon + a_0$$

where a_4, a_3, a_2, a_1, and a_0 are constants determined through curve fitting to the experimental data.

This polynomial fitting allowed for a more accurate representation of the material's behavior beyond the elastic limit, where the response of the specimen to the applied force no longer followed a simple linear pattern. Once the polynomial curve was fitted to the data, it was differentiated to obtain its derivative.

$$\frac{d\sigma}{d\epsilon} = 4a_4\epsilon^3 + 3a_3\epsilon^2 + 2a_2\epsilon + a_1$$

The maximum value of this derivative provides insight into the material's peak elastic modulus, which is a measure of how the material's stiffness evolves as it undergoes plastic deformation. In soft tissues, this modulus is particularly relevant for understanding how the tissue resists further deformation once it has been stretched beyond its elastic limit. This approach allows for a more detailed analysis of the mechanical behavior in the plastic region, especially in cases where the material exhibits complex, nonlinear responses.

Below are some indicative initial force-displacement diagrams, along with the fitting parameters of the polynomial curve obtained from the analysis software. Additionally, the diagram of the first derivative of the polynomial curve is provided. The maximum point of this derivative curve was defined as the peak elastic modulus.

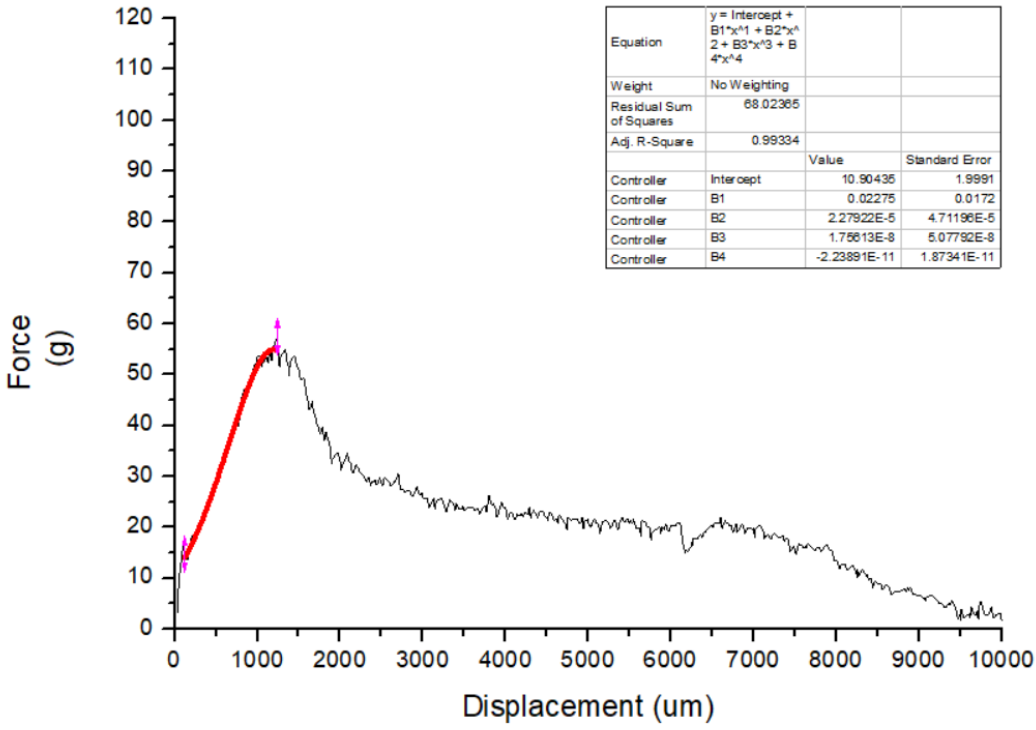

Equation	y = Intercept + B1*x^1 + B2*x^2 + B3*x^3 + B4*x^4		
Weight	No Weighting		
Residual Sum of Squares	68.02365		
Adj. R-Square	0.99334		
		Value	Standard Error
Controller	Intercept	10.90435	1.9991
Controller	B1	0.02275	0.0172
Controller	B2	2.27922E-5	4.71196E-5
Controller	B3	1.75613E-8	5.07792E-8
Controller	B4	-2.23891E-11	1.87341E-11

Figure 10: Force-Displacement graph, along with the fitting parameters of the polynomial curve obtained from the analysis software for specimen 7a7out.

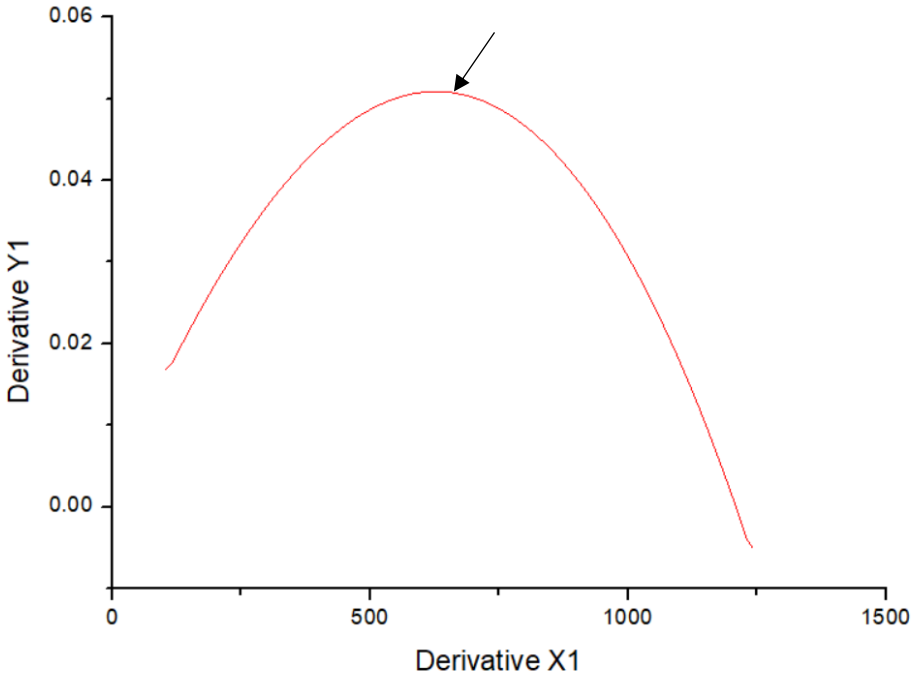

Figure 11: First derivative of the polynomial curve of specimen 7a7out. The maximum point is depicted.

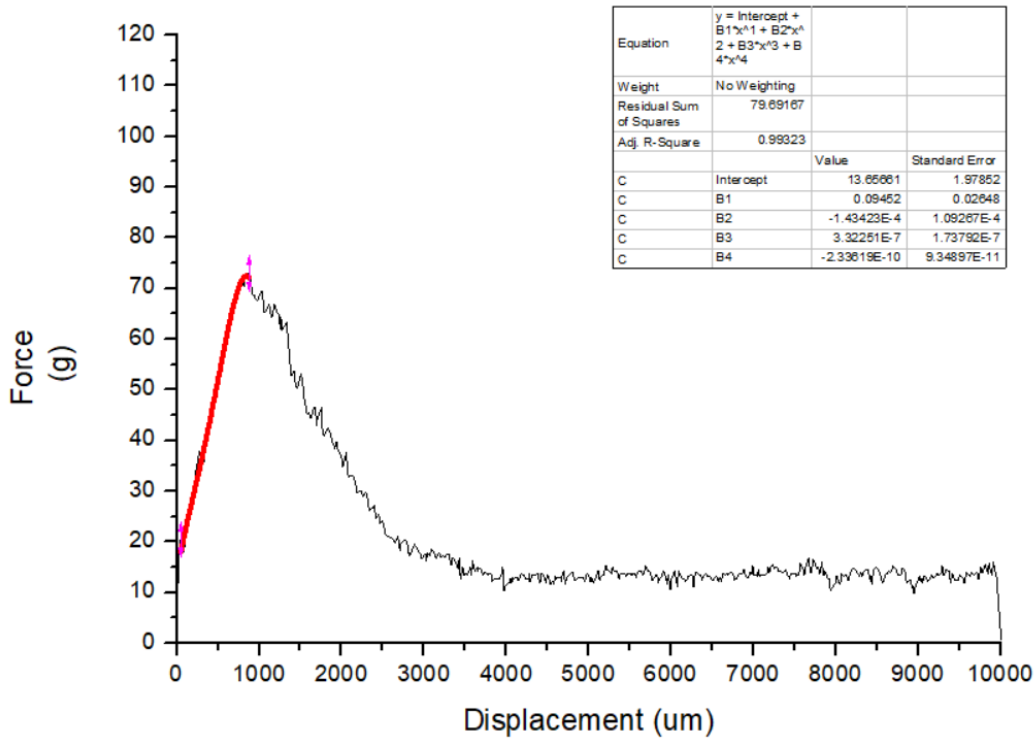

Figure 12: Force-Displacement graph, along with the fitting parameters of the polynomial curve obtained from the analysis software for specimen 10a2out.

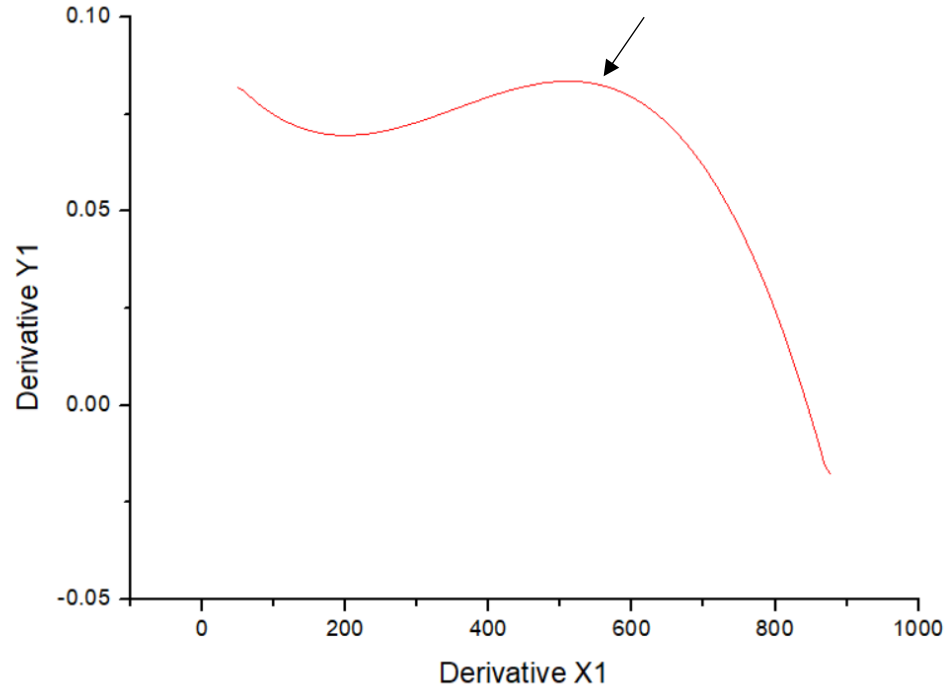

Figure 13: First derivative of the polynomial curve of specimen 10a2out. The maximum point is depicted.

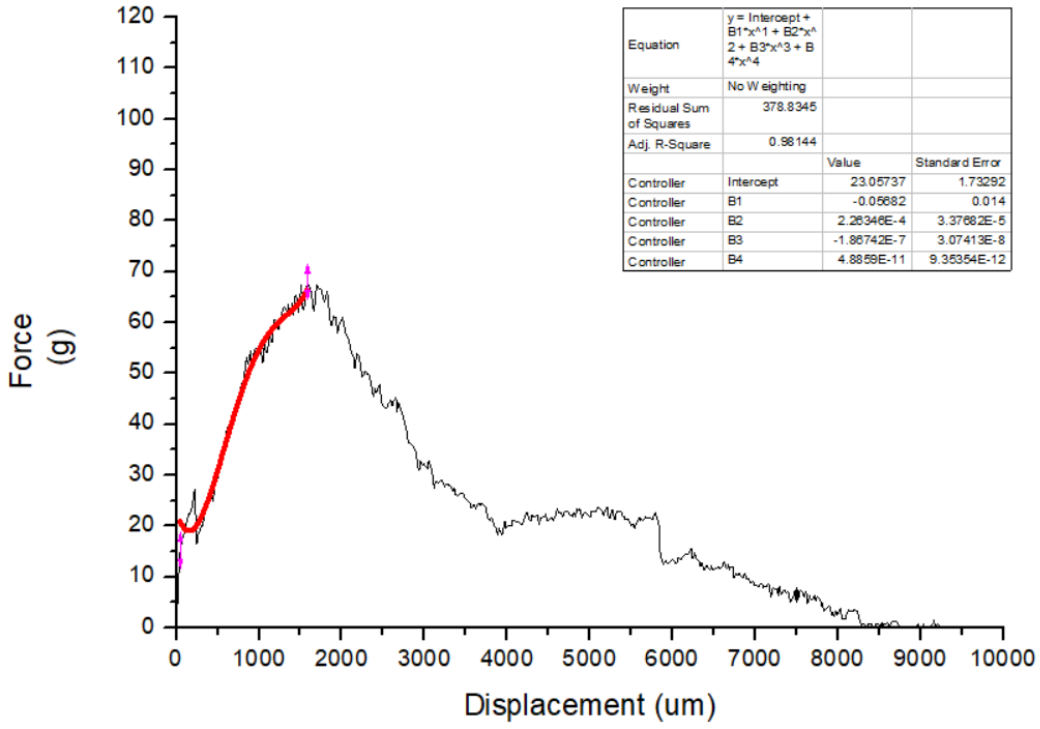

Figure 14: Force-Displacement graph, along with the fitting parameters of the polynomial curve obtained from the analysis software for specimen 11rl8out.

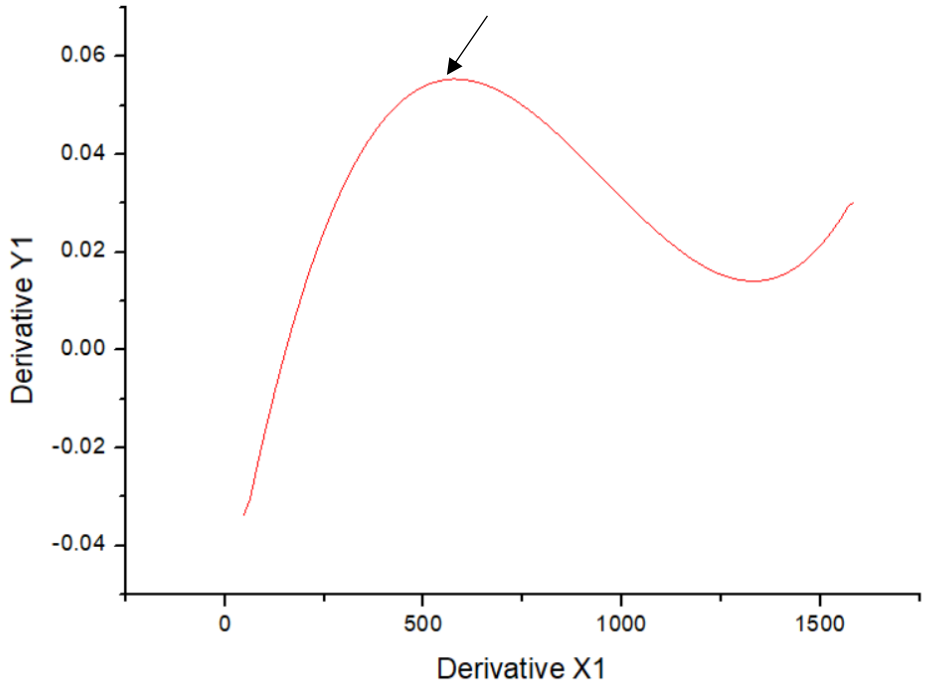

Figure 15: First derivative of the polynomial curve of specimen 11rl8out. The maximum point is depicted.

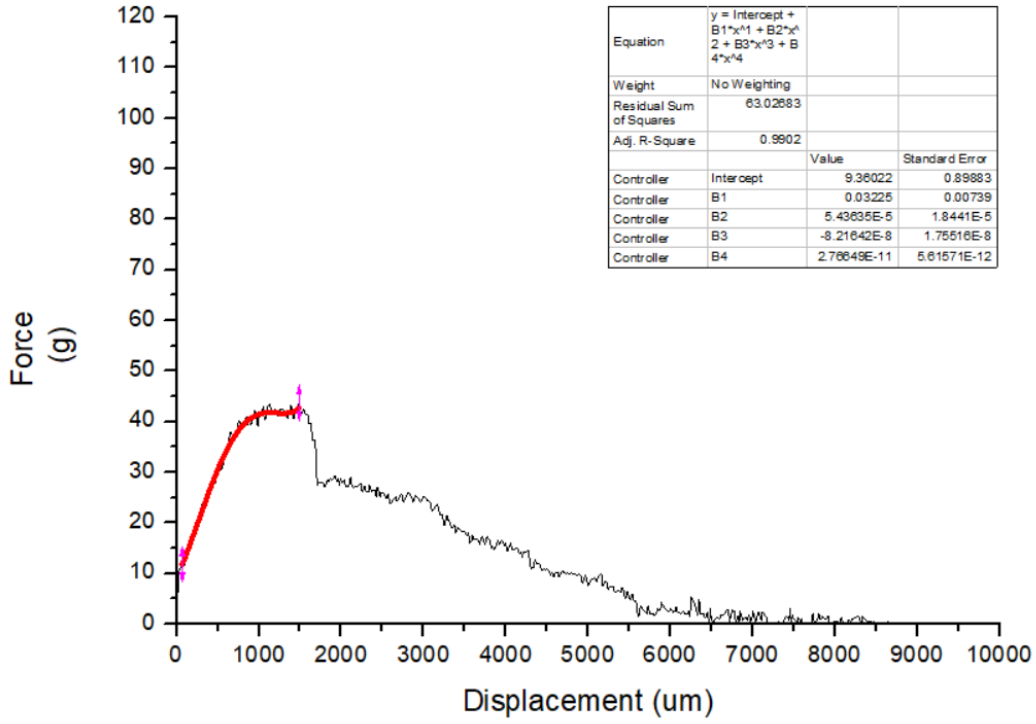

Equation	y = Intercept + B1*x^1 + B2*x^2 + B3*x^3 + B4*x^4		
Weight	No Weighting		
Residual Sum of Squares	63.02683		
Adj. R-Square	0.9902		
		Value	Standard Error
Controller	Intercept	9.36022	0.89883
Controller	B1	0.03225	0.00739
Controller	B2	5.43635E-5	1.8441E-5
Controller	B3	-8.21642E-8	1.75516E-8
Controller	B4	2.76649E-11	5.61571E-12

Figure 16: Force-Displacement graph, along with the fitting parameters of the polynomial curve obtained from the analysis software for specimen 1rl8out.

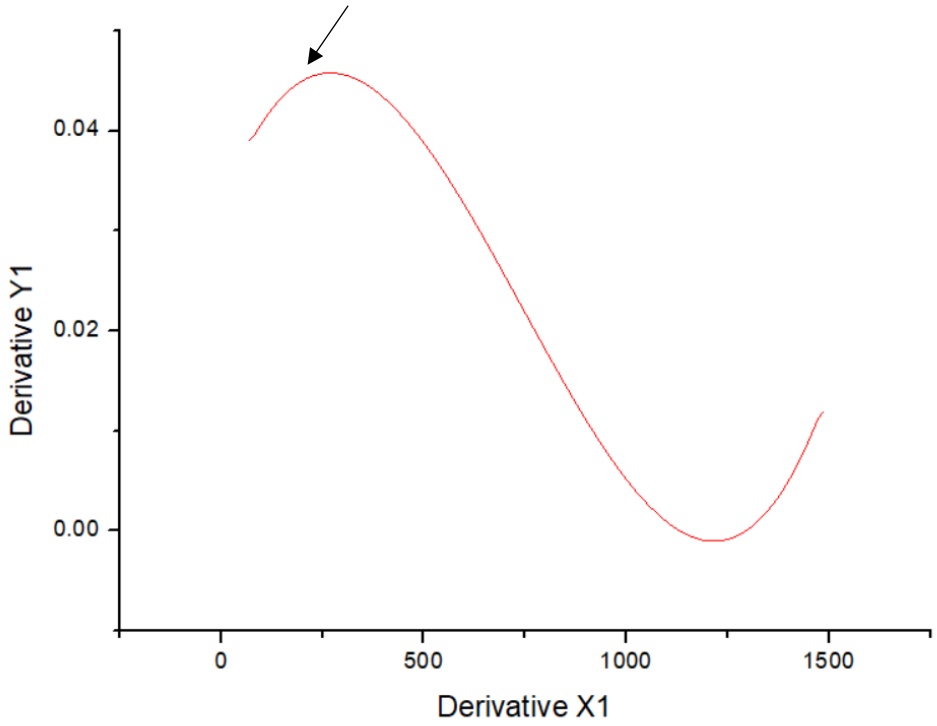

Figure 17: First derivative of the polynomial curve of specimen 1rl8out. The maximum point is depicted.

Results

Maximum force (F_{max}) for each specimen

In this study, the mechanical properties of aortic wall specimens were assessed through two distinct incisions: one made between the intima and media layers (inner incision), and the other between the media and adventitia layers (outer incision). This approach was designed to study the propagation of rupture across the different layers within the aortic wall and how they respond to mechanical stress up to the point where the force reaches zero. By focusing on the maximum force (F_{max}) at tissue failure for each specimen, the analysis provides valuable insights into the mechanical strength of the aortic wall based on the location of the incision.

A total of 74 specimens were tested, divided into two groups: 35 specimens for the inner incision and 39 for the outer incision. The two graphs presented below depict the F_{max} values recorded for each specimen and the average F_{max} for the respective groups. The first graph illustrates the maximum force at failure for each specimen following an inner incision, while the second graph focuses on specimens where failure occurred following an outer incision. These visual representations highlight the variability in mechanical strength across all tested samples, emphasizing how the aortic wall performs differently depending on the anatomical layers involved in the failure process and each patient's characteristics.

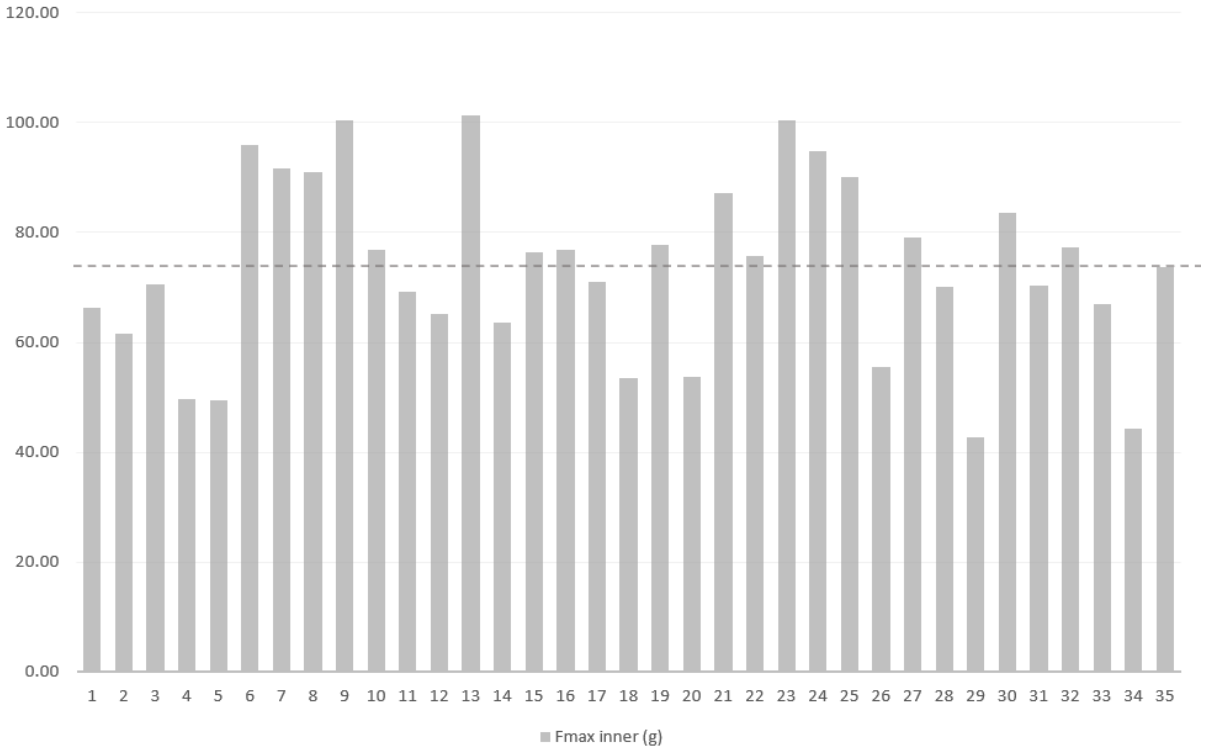

Figure 18: Maximum force (F_{max}) recorded for each specimen when the initial incision is taking place between the intima and media layers (inner)

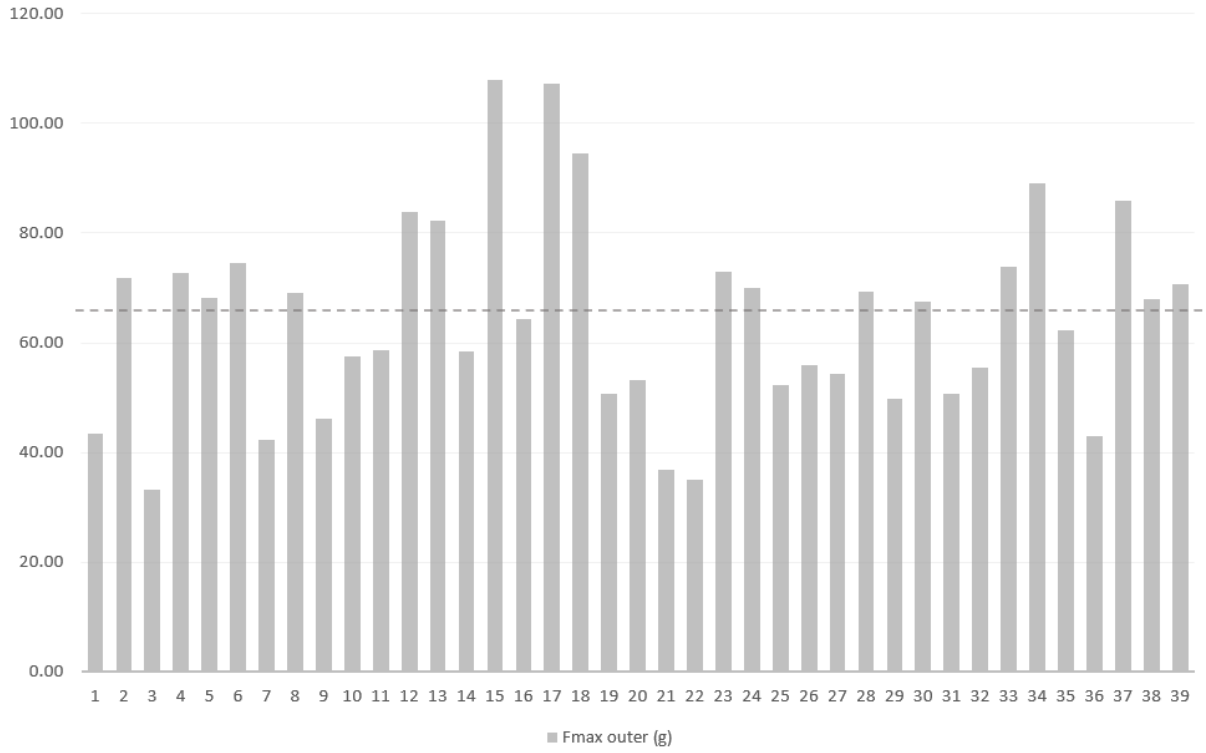

Figure 19: Maximum force (F_{max}) recorded for each specimen when the initial incision is taking place between the media and adventitia layers (outer)

The results of the mechanical tests reveal distinct differences in the performance of aortic wall specimens based on the location of the incision. For specimens with an **inner incision**, the maximum force at failure (F_{max}) ranged **from 42.75g to 101.25g,** with an average of 73.53g and a standard deviation of 16.27g. This indicates a relatively consistent performance in terms of mechanical strength for this group, with most values clustered around the average. The spread of data suggests that the mechanical properties of the aortic wall in this region may be more uniform among the specimens tested.

In contrast, the specimens with an **outer incision**, where rupture occurred between the media and adventitia layers, exhibited a wider range of F_{max} values, **from 33.25g to 108g**, with a lower average of 64.18g and a higher standard deviation of 18.13g. This suggests greater variability in the mechanical properties of the aortic wall when the outer layers are involved. The wider range and higher variability in the outer incision group could reflect heterogeneity in the structure and mechanical performance of the outer layers of the aorta among different specimens.

The comparison between the two groups shows that, on average, specimens with an inner incision exhibited higher mechanical resistance to failure than those with an outer incision. This suggests that the aortic wall may be more resistant to mechanical stress when failure is initiated between the intima and media layers compared to the media and adventitia layers. Additionally, the greater variability observed in the outer incision group points to more inconsistent mechanical behavior in the outer regions of the aortic wall.

Comparison between layers and anatomical regions

Force - Displacement Curves

For the direct tension test, a total of 74 force-displacement curves were gathered to capture the mechanical behavior of the aortic wall specimens during radial extension. These curves represent the progression of mechanical forces applied to the coin-shaped specimens up to the point where the force reaches zero. The specimens were categorized by the type of incision—either inner (between the intima and media) or outer (between the media and adventitia)—as well as by their anatomical position within the aorta: left lateral (LL), right lateral (RL), anterior (A), and posterior (P). Due to the anatomical shape of the left lateral region, fewer specimens were available from this area, which impacted the total number of curves collected from it. Thus, eight different groups of curves were analyzed, corresponding to each region and incision type.

	Inner	Outer
Anterior	10	11
Right Lateral	13	15
Posterior	6	9
Left Lateral	6	4

Table 2: Number of specimens for each incision type and anatomical region within the aorta

To visualize the overall mechanical performance for each of these groups, an average curve was calculated using data processing software, OriginPro 8.5. This average curve, represented by a thick and solid red line, was computed from the collected data and provides a general depiction of how the tissue responds under tension for each layer and region. After the complete separation of a specimen, the force dropped to zero, reaching what is referred to as the zero-load level. This final point corresponds to a specific radial displacement, which varied across the specimens. Notably, each individual test concluded at a different point on the displacement axis, ranging from approximately 3.2mm to 12.2mm. Despite this variability, the mean curve was extended beyond the first specimen's ending point to ensure consistency in the comparison.

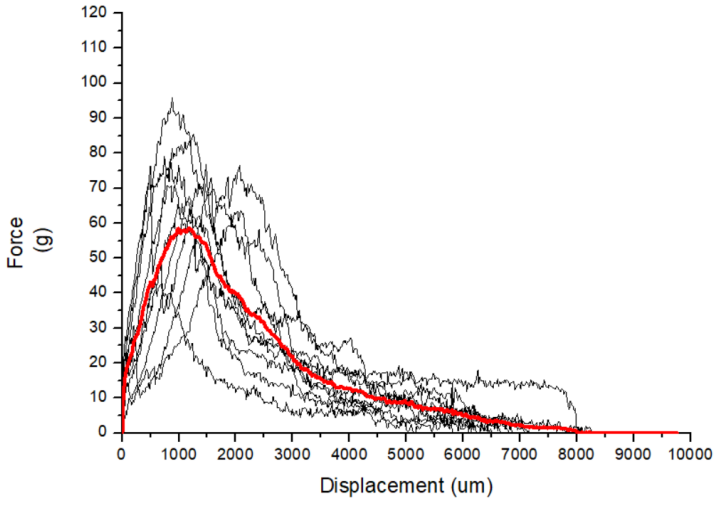

Figure 20: Force-displacement curves for the specimens from the anterior region with an inner incision.

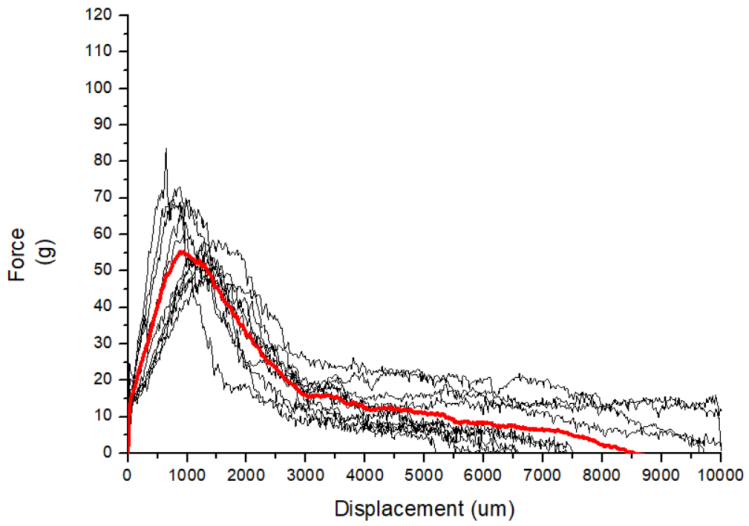

Figure 21: Force-displacement curves for the specimens from the anterior region with an outer incision.

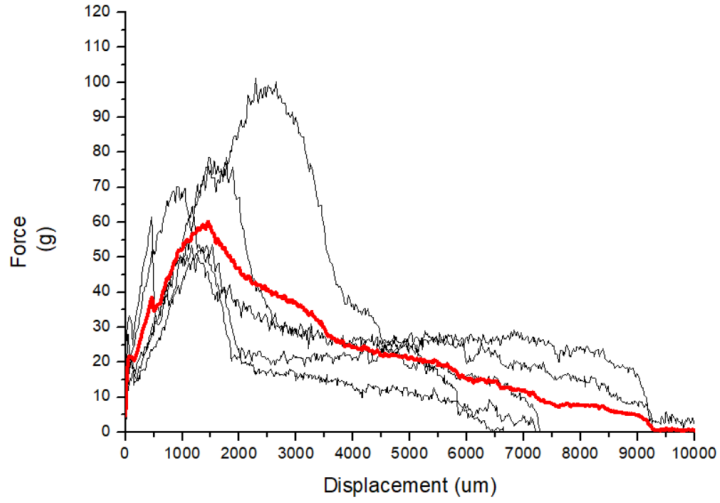

Figure 22: Force-displacement curves for the specimens from the left lateral region with an inner incision.

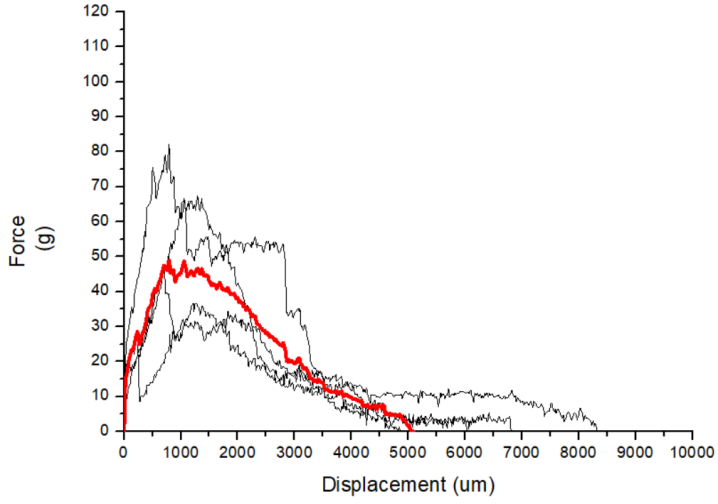

Figure 23: Force-displacement curves for the specimens from the left lateral region with an outer incision.

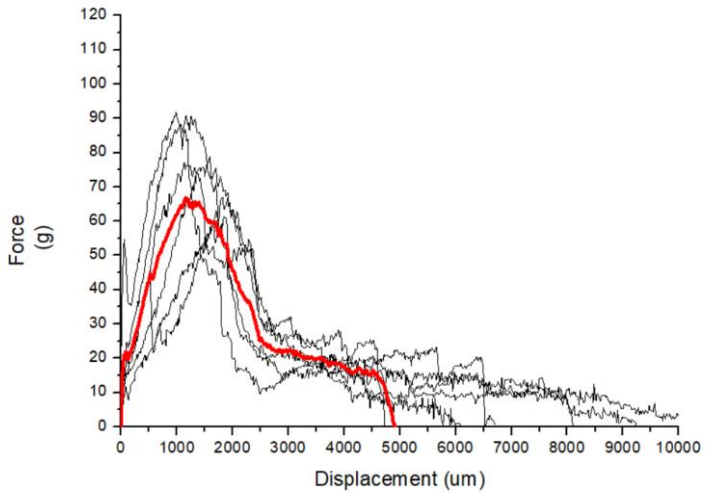

Figure 24: Force-displacement curves for the specimens from the posterior region with an inner incision.

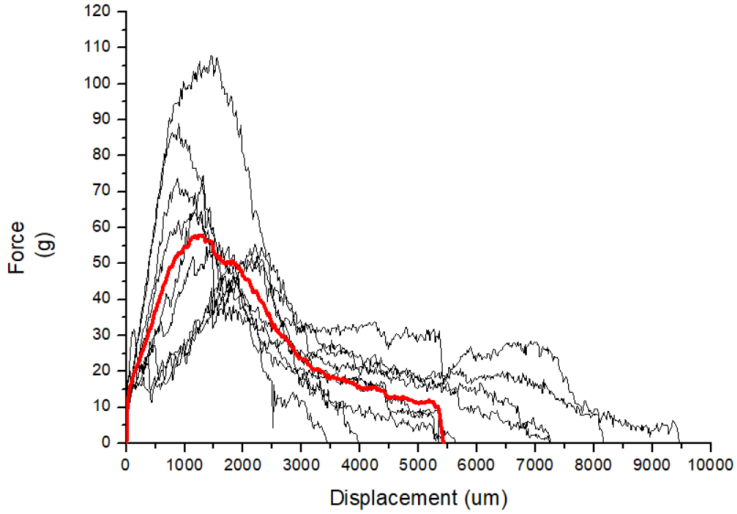

Figure 25: Force-displacement curves for the specimens from the posterior region with an outer incision.

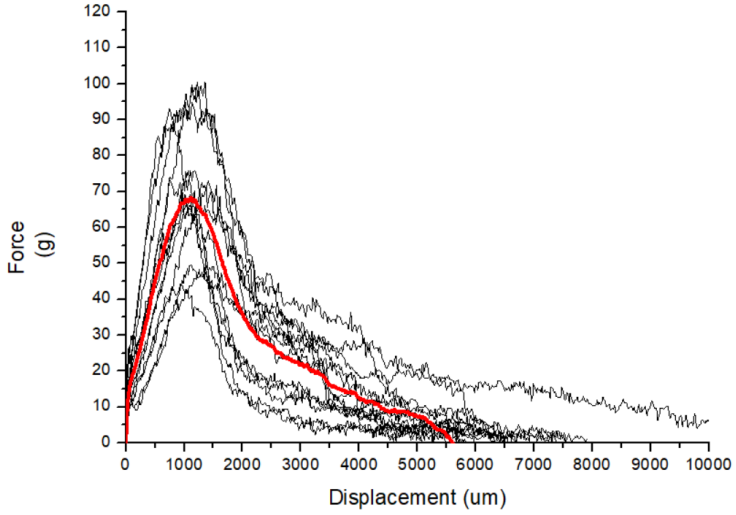

Figure 26: Force-displacement curves for the specimens from the right lateral region with an inner incision.

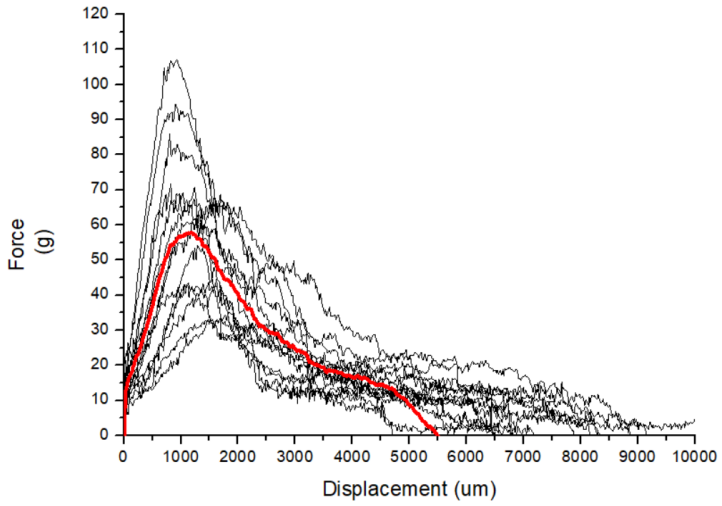

Figure 27: Force-displacement curves for the specimens from the right lateral region with an outer incision.

Yield Force (F_{yield})

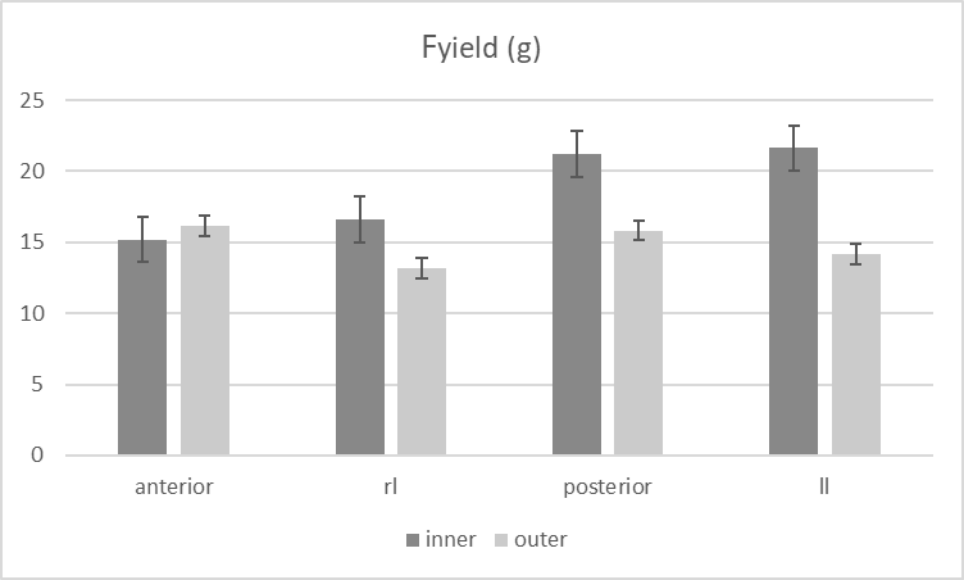

Figure 28: Comparison of Yield Force (F_{yield}) across aortic wall regions and layers.

The plot reveals significant differences in the mechanical properties of the aortic wall across the four anatomical regions and between the inner and outer layers.

The **left lateral (ll) region** presents the highest F_{yield} value for the inner layer, with a yield force of **21.63 g**. This suggests that the intima-media interface in this region has the greatest resistance to rupture initiation under tensile loading. The outer layer in this region, however, shows a much lower F_{yield} of **14.17 g**, indicating that the media-adventitia interface is more prone to rupture. The large difference between the inner and outer layers in the left lateral region suggests a significant mechanical disparity, with the inner layers playing a more dominant role in resisting rupture.

The **posterior region** also exhibits high F_{yield} values for the inner layer at **21.19 g**, close to the left lateral region. The outer layer in the posterior region has a lower F_{yield} of **15.84 g**, showing that, while still relatively strong, the outer layer in this region is not as resistant to rupture as the inner layer. The smaller difference between the inner and outer layers in the posterior region compared to the left lateral region indicates that both layers contribute more evenly to the mechanical resistance of the aortic wall in this area.

In the **anterior region**, the inner layer has an F_{yield} of **15.21 g**, and the outer layer shows a slightly higher value at 16.18 g. This suggests that in this region, the outer layer (media-adventitia) is marginally stronger than the inner layer (intima-media) in resisting rupture initiation. The relatively close values between the two layers indicate a more uniform mechanical response across the wall in the anterior region compared to the other regions.

The **right lateral (rl) region** presents the lowest F_{yield} value for the outer layer, at **13.15 g**, suggesting that the media-adventitia interface is the weakest in this region and more prone to rupture under tensile loading. The inner layer in this region has a moderately higher Fyield of **16.58 g**, indicating that the intima-media interface is stronger than the outer layer but still not as resistant as the posterior or left lateral inner layers.

In summary, the left lateral region has the highest Fyield for the inner layer, reflecting its superior resistance to rupture, while the right lateral region has the lowest Fyield for the outer layer, suggesting that it is more vulnerable. The posterior region also shows high resistance in the inner layer, while the anterior region presents more balanced mechanical properties between the inner and outer layers. These variations highlight the complexity of rupture behavior in different regions of the aneurysmatic aorta and the distinct roles that the inner and outer layers play in mechanical resistance.

Elastic Modulus

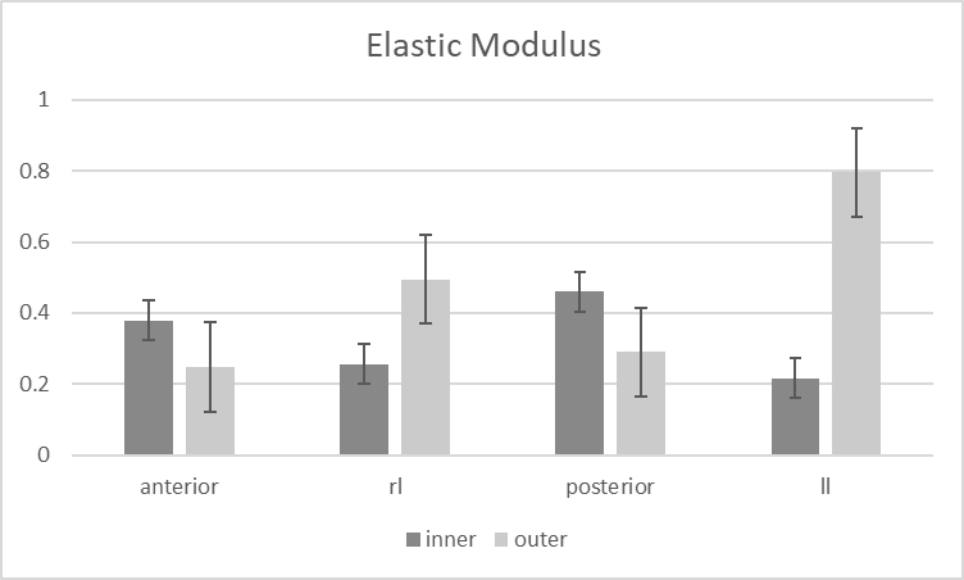

Figure 29: Comparison of Elastic Modulus across aortic wall regions and layers.

For the elastic modulus plot, we observe differences between the inner and outer layers across the various aortic regions, reflecting their stiffness in the elastic region of deformation.

In the **posterior region**, the inner layer exhibits the highest elastic modulus at **0.50**, suggesting that this layer is the stiffest and offers the greatest resistance to initial deformation. The outer layer in this region has a lower elastic modulus of **0.29**, indicating that the media-adventitia boundary is more compliant compared to the intima-media boundary. The significant difference between the two layers implies that, in the posterior region, the inner layer plays a more dominant role in maintaining structural integrity during the initial elastic phase of loading.

In the **left lateral region**, the outer layer has the **highest elastic modulus overall**, with a value of **0.80**, indicating a very stiff outer structure in this region. In contrast, the inner layer in the left lateral region has a much lower elastic modulus of **0.22**, which is the lowest among all regions. This large discrepancy between the inner and outer layers suggests that in the left lateral region, the outer layer is responsible for resisting initial deformation, while the inner layer is much more compliant, indicating a high degree of flexibility or vulnerability in the intima-media interface.

The **right lateral region** presents an interesting contrast, with the outer layer showing a relatively high elastic modulus of **0.50**, which is greater than the inner layer's value of **0.26**. This indicates that, in the right lateral region, the outer layer is stiffer and more resistant to elastic deformation than the inner layer, a reversal of the trend seen in other regions where the inner layer is often stronger. This suggests that the media-adventitia interface in this region is crucial for maintaining the mechanical stability of the aortic wall.

In the **anterior region**, the inner layer has a higher elastic modulus of **0.38**, compared to the outer layer's value of **0.25**. This implies that, in the anterior region, the intima-media boundary is stiffer and more resistant to elastic deformation than the outer media-adventitia boundary. The relatively small difference between the two layers suggests a more uniform distribution of mechanical properties, where both layers contribute to resisting deformation, though the inner layer plays a slightly stronger role.

In summary, the left lateral region exhibits the highest outer elastic modulus, indicating significant stiffness in the outer layer, although this observation is based on the smallest sample size among all groups. The posterior region shows the highest inner elastic modulus, reflecting greater stiffness in the inner layer. The anterior region

presents a moderate difference between the inner and outer layers, with the inner layer being stiffer, while the right lateral region demonstrates the opposite trend, where the outer layer is stiffer than the inner. These variations in elastic modulus across different regions underscore the complex mechanical behavior of the aortic wall, where both the inner and outer layers contribute differently depending on the anatomical location.

Maximum Force (F_{max})

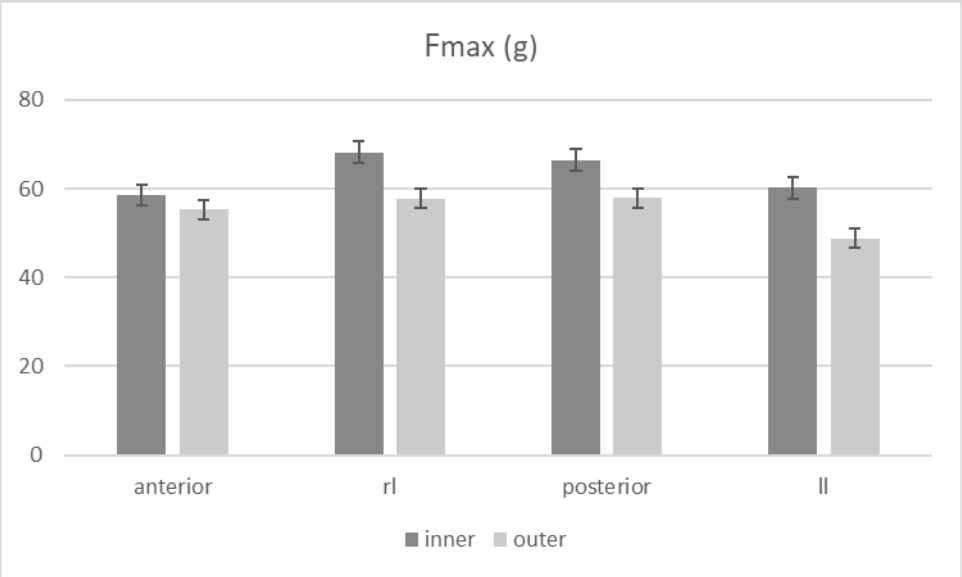

Figure 30: Comparison of F_{max} across aortic wall regions and layers.

The graph presents the maximum force (F_{max}) values in grams for both inner and outer layers across different anatomical regions of the aortic wall: anterior, right lateral (rl), posterior, and left lateral (ll). F_{max} represents the maximum force the tissue can withstand before failure, providing insight into the mechanical strength of each region. Notable differences are observed between the inner and outer layers across the four anatomical regions, reflecting their strength under tensile loading.

In the **right lateral (rl) region**, the inner layer exhibits the **highest F_{max}** at **68.22g**, suggesting that the intima-media interface in this region is the strongest and most resistant to rupture under maximum tensile forces. The outer layer in the right lateral region has a significantly lower F_{max} of **57.83g**, indicating that the media-adventitia interface is less capable of sustaining high forces before failure. The substantial difference between the two layers shows that the inner layer plays a more critical role in resisting rupture in this region.

In the **posterior region**, the inner layer also shows a high F_{max} value of **66.52g**, slightly lower than the right lateral region, but still reflecting strong mechanical resistance. The outer layer in the posterior region has a lower F_{max} of **57.91g**, indicating that the outer part of the aortic wall is less resistant to rupture compared to the inner layer. The difference between the inner and outer layers in this region suggests that the inner portion is the primary contributor to strength under maximal loading, similar to the right lateral region.

In the **left lateral (ll) region**, the inner layer has a moderate F_{max} of **60.20g**, while the outer layer shows a much lower F_{max} of **48.85g**. This significant difference indicates that the inner layer in the left lateral region is much stronger than the outer layer, which appears to be the weakest among all regions studied. The outer layer's low F_{max} suggests that the media-adventitia interface in this region is particularly vulnerable to rupture under tensile forces.

In the **anterior region**, both the inner and outer layers exhibit more comparable F_{max} values, with the inner layer showing **58.53g** and the outer layer slightly lower at **55.26g**. The relatively small difference between the two layers in this region indicates that both the intima-media and media-adventitia interfaces contribute fairly evenly to resisting tensile forces before failure. This balance between the layers suggests a more uniform mechanical strength across the aortic wall in the anterior region compared to the other regions.

In summary, the right lateral region demonstrates the highest F_{max} for the inner layer, indicating the strongest resistance to rupture, while the left lateral region shows the lowest F_{max} for the outer layer, making it the most vulnerable. The posterior region also shows high resistance in the inner layer, while the anterior region displays more balanced values between the inner and outer layers. These variations in F_{max} across regions highlight the distinct mechanical behavior of the aortic wall, with certain regions showing a stronger inner layer and others a more balanced distribution of strength between the inner and outer layers.

Peak Elastic Modulus (PEM)

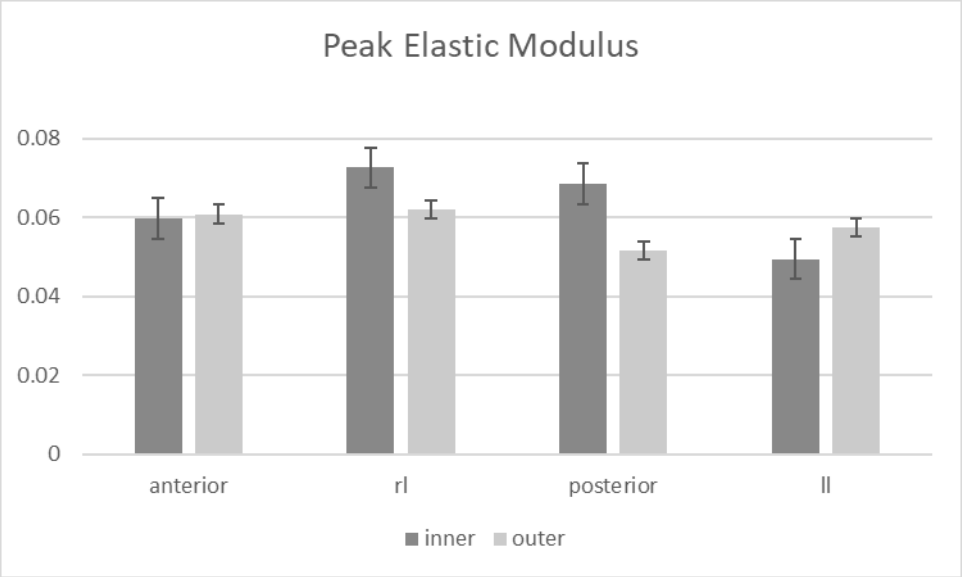

Figure 31: Comparison of Peak Elastic Modulus across aortic wall regions and layers.

For the Peak Elastic Modulus (PEM) plot, which represents the maximum stiffness of the tissue during plastic deformation, there are notable differences across the anatomical regions between the inner and outer layers.

In the **right lateral (rl) region**, the inner layer shows the **highest PEM** at **0.073**, indicating that during the plastic phase of deformation, the intima-media boundary in this region is stiffer than in other regions. This suggests that even after yielding, the inner layer in the right lateral region resists further deformation effectively. The outer layer in this region has a lower PEM of **0.062**, indicating that it is less stiff during plastic deformation than the inner layer, though still relatively strong compared to other regions.

The **posterior region** also exhibits a high PEM for the inner layer, with a value of **0.069**, which is slightly lower than in the right lateral region but still reflects significant stiffness during plastic deformation. The outer layer in the posterior region has a PEM of **0.052**, which is the lowest among all regions, suggesting that the media-adventitia boundary in the posterior region is the least resistant to deformation during the plastic phase, making it more vulnerable as deformation progresses.

In the **anterior region**, the inner and outer layers show very similar PEM values, with the inner layer at **0.060** and the outer layer at **0.061**. This small difference indicates that both layers exhibit almost identical stiffness during plastic deformation in the anterior region. The balance between the inner and outer layers here suggests a uniform mechanical behavior during plastic deformation, with both layers contributing equally to resisting further deformation.

In the **left lateral (ll) region**, the inner layer shows the **lowest PEM** overall, with a value of **0.050**, indicating that the intima-media boundary in this region is the most compliant during plastic deformation. The outer layer, however, exhibits a higher PEM of **0.058**, suggesting that in the left lateral region, the media-adventitia boundary plays a more significant role in resisting deformation during the plastic phase, a reversal of the pattern seen in other regions.

In summary, the right lateral region demonstrates the highest PEM for the inner layer, indicating strong resistance to plastic deformation, while the posterior region has the lowest PEM for the outer layer, making it more prone to deformation as it progresses through the plastic phase. The anterior region shows a balanced mechanical response between the inner and outer layers, with nearly identical stiffness during plastic deformation, while the left lateral region presents the opposite trend, with the outer layer being stiffer than the inner. These regional differences in PEM highlight the varying mechanical behaviors of the aortic wall during plastic deformation, where certain layers dominate in stiffness depending on the anatomical region.

Stretch

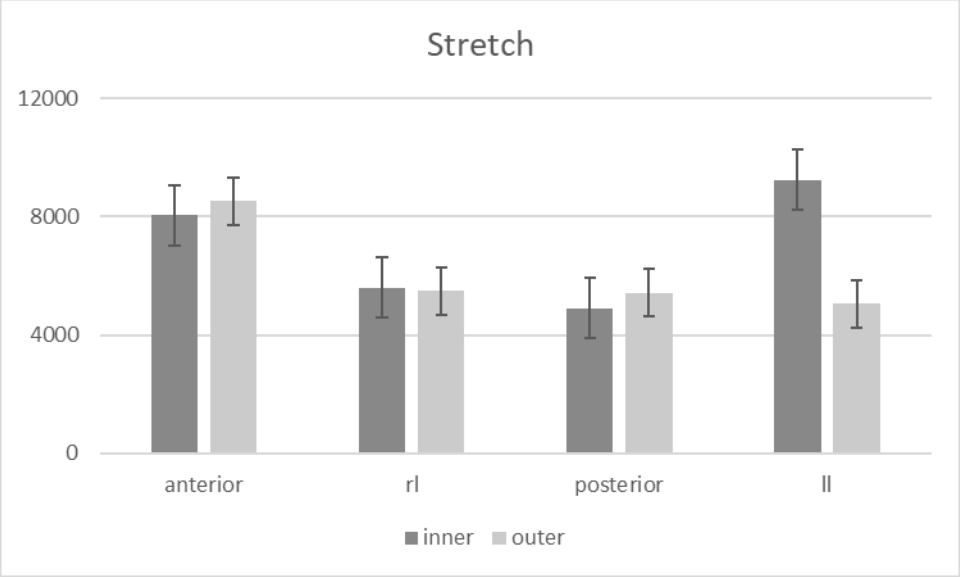

Figure 32: Comparison of Stretch across aortic wall regions and layers.

For the stretch plot, which reflects the maximum displacement before rupture, we observe differences across the anatomical regions for the inner and outer layers, indicating their capacity for elongation under tensile loading.

In the **left lateral (ll) region**, the inner layer demonstrates the **highest stretch**, with a max value of **9,0mm**, indicating that this layer is the most compliant and capable of significant elongation before rupture. The outer layer in this region shows a much lower max of **5,0mm**, suggesting that the media-adventitia boundary in the left lateral region has a much lower capacity for stretch before failure. The stark difference between the inner and outer layers highlights that in the left lateral region, the inner layer is considerably more ductile, whereas the outer layer is much stiffer and prone to rupture earlier.

In the **anterior region**, the outer layer shows the **highest stretch for outer layers** among all regions, with a max of **8,5mm**, while the inner layer has a slightly lower value of **8,0mm**. This suggests that in the anterior region, the outer media-adventitia interface has a greater capacity for elongation before failure compared to the inner layer, which contrasts with the behavior seen in most other regions. The relatively small difference between the inner and outer layers suggests a more uniform distribution of strain across the wall in the anterior region.

In the **right lateral (rl) region**, the inner layer has a max of **5,6mm**, while the outer layer shows a very similar value of **5,5mm**. The minimal difference between these values indicates that there is no statistically significant difference in the stretch capacity between the inner and outer layers in this region. Both the intima-media and media-adventitia interfaces exhibit nearly equal compliance and capacity for elongation before rupture. This suggests that, in the right lateral region, the mechanical behavior of the aortic wall is uniform across the inner and outer layers when it comes to tensile loading and elongation, and neither layer demonstrates a dominant role in resisting deformation before rupture.

In the **posterior region**, the outer layer exhibits a higher max value of **5,5mm** compared to the inner layer's value of **4,9mm**. This suggests that in the posterior region, the outer layer has a greater capacity for stretch before rupture, contrasting with the behavior in the left lateral and right lateral regions. The relatively low values in both layers indicate that the posterior region is the least compliant overall, with both the inner and outer layers being more prone to rupture under tensile forces without significant elongation.

In summary, the left lateral region shows the highest stretch for the inner layer, indicating a high capacity for elongation before rupture, while the outer layer in this region is much less compliant. The anterior region exhibits the highest stretch for the outer layer, with both layers showing significant elongation before failure. The right lateral region demonstrates moderate stretch values for both layers, with the inner layer being slightly more compliant, while the posterior region shows the lowest stretch, with both layers being more prone to rupture with minimal elongation. These variations in stretch across regions reflect the differing capacities of the aortic wall layers to accommodate deformation before rupture, with certain regions demonstrating more ductility than others.

Stress and strain behavior

region and layer of aortic wall	Elastic Region (S1)		Plastic Region (S2)		Ending Point (S3)
	σ (N/cm2)	ε	σ (N/cm2)	ε	ε
Anterior-inner	0.80 ± 0.33	0.05 ± 0.03	2.53 ± 0.51	0.59 ± 0.22	3.26 ± 0.60
Anterior-outer	0.76 ± 0.19	0.07 ± 0.06	2.24 ± 0.39	0.49 ± 0.13	3.56 ± 0.92
RL- inner	0.71 ± 0.29	0.05 ± 0.03	2.59 ± 0.67	0.50 ± 0.08	2.97 ± 0.63
RL- outer	0.58 ± 0.18	0.03 ± 0.01	2.24 ± 0.77	0.54 ± 0.13	3.42 ± 1.01
Posterior – inner	0.84 ± 0.55	0.04 ± 0.01	2.71 ± 0.49	0.59 ± 0.16	3.32 ± 0.99
Posterior – outer	0.89 ± 0.98	0.08 ± 0.12	2.43 ± 0.72	0.73 ± 0.25	3.00 ± 1.18
LL-inner	0.82 ± 0.22	0.03 ± 0.01	2.62 ± 0.67	0.60 ± 0.26	3.25 ± 1.17
LL-outer	0.85 ± 0.30	0.05 ± 0.04	2.06 ± 0.73	0.40 ± 0.12	2.55 ± 0.60

Table 3: Stress and Strain values across aortic wall regions and layers.

The table reveals crucial insights into the mechanical behavior of the aortic wall, particularly in understanding the propagation of rupture between the layers (inner vs. outer) and the regional variations within the aorta.

The **anterior region** demonstrates a relatively balanced mechanical response between the inner and outer layers. In the plastic region (S2), the inner layer exhibits a stress value of 2.53 ± 0.51 N/cm², while the outer layer shows a slightly lower value of 2.24 ± 0.39 N/cm². The difference in stress between the layers suggests that the inner layer is better equipped to bear mechanical loads before reaching its yield point, which is important in withstanding pressures from the cardiac cycle.

Strain values follow a similar trend, with the inner layer showing slightly higher deformation capabilities compared to the outer layer in the plastic region. This balance between stress and strain across layers highlights the anterior region's ability to handle moderate to high mechanical stress before failure. It is mechanically stable but not as robust as the posterior region in terms of ultimate stress-bearing capacity.

In the **right lateral (RL) region**, the mechanical properties are moderate. Both the stress and strain values are lower than in the anterior and posterior regions, particularly in the outer layer. In the plastic region (S2), the RL outer layer exhibits a stress value of 2.24 ± 0.77 N/cm², lower than in the anterior and posterior regions, indicating that this region may have a slightly reduced ability to bear mechanical loads, particularly in the outer layer. However, the RL region's inner layer shows higher mechanical strength than its outer layer, suggesting that the inner layer plays a significant role in bearing mechanical stress.

The **posterior region stands out as the most mechanically resilient**. Both the inner and outer layers in this region show the highest stress values, particularly in the plastic region (S2), where the posterior inner layer has a stress of 2.71 ± 0.49 N/cm². Additionally, the strain values are relatively high, indicating that the posterior region is capable of withstanding considerable deformation before failure. This makes the posterior region particularly robust, as it can absorb significant stress while maintaining structural integrity. The high strain capacity further suggests that the posterior region is adaptable and able to handle gradual deformation, helping distribute mechanical forces over time and delaying the onset of rupture.

The **left lateral (LL) region** displays an intermediate mechanical profile, with stress values higher than those in the right lateral region but lower than those in the posterior. In the plastic region, the inner layer has a stress of 2.62 ± 0.67 N/cm², while the outer layer shows 2.06 ± 0.73 N/cm². This suggests that the left lateral region can bear moderate stress loads before rupture but is not as resistant as the posterior region.

Strain values in the left lateral region show moderate deformation capacity, with the outer layer showing a strain of 2.55 ± 0.60 in the ending point (S3), lower than the anterior or posterior regions. This lower strain in the final stages of deformation may suggest that the left lateral region could become more vulnerable during the later stages of stress application, possibly contributing to gradual mechanical failure.

When analyzing the **inner and outer layers overall**, it is evident that the inner layer tends to exhibit higher stress values across most regions, suggesting that it plays a crucial role in resisting mechanical forces. However, the

inner layer is also generally more deformable, as indicated by the higher strain values in many regions. This points to a trade-off where the inner layer, while stronger, is also more elastic. In contrast, the outer layer, particularly in regions like the rl and ll, demonstrates lower stress resistance but greater stiffness, as evidenced by lower strain values. The outer layer appears to function as a more rigid barrier, preventing excessive deformation but potentially at the cost of reduced flexibility and higher vulnerability to failure under extreme conditions.

Patients' characteristics influence on mechanical properties

inner													
#	Gender	Age	Valve Type	S1				S2				S3	
				σ (N/cm2)		ε (-)		σ (N/cm2)		ε (-)		ε (-)	
				mean	sd	mean	sd	mean	sd	mean	sd	mean	sd
1	F	67	TAV	0.62	0.23	0.04	0.01	2.10	0.34	0.54	0.08	2.85	0.62
2	M	50	TAV	1.14	0.54	0.03	0.01	3.35	0.16	0.49	0.07	3.10	0.65
3	M	54	TAV	0.64	0.13	0.03	0.01	2.58	0.19	0.55	0.14	3.33	1.10
5	M	33	TAV	0.59	0.00	0.03	0.00	2.31	0.00	0.46	0.00	2.68	0.00
6	M	74	TAV	1.18	0.00	0.03	0.00	3.58	0.00	1.07	0.00	3.39	0.00
7	M	76	BAV	0.72	0.29	0.05	0.03	2.67	0.53	0.61	0.18	3.26	0.75
8	M	37	TAV	1.05	0.00	0.05	0.00	3.18	0.00	0.42	0.00	3.89	0.00
9	F	56	TAV	0.42	0.00	0.03	0.00	1.96	0.00	0.61	0.00	4.46	0.00
10	M	53	TAV	0.92	0.53	0.07	0.01	2.63	0.23	0.48	0.22	2.72	0.17
11	M	55	BAV	0.75	0.29	0.05	0.03	2.32	0.56	0.50	0.20	3.07	1.10
12	M	54	TAV	-	-	-	-	-	-	-	-	-	-

Table 4: Patient Characteristics and Stress-Strain values for inner incision.

The mechanical properties of the specimens derived from different patients appear to show significant variation, influenced by factors such as age, gender, and valve type. Age seems to be an important determinant of tissue mechanics, with younger patients often exhibiting higher stress values in both the elastic (S1) and plastic (S2) regions of the stress-strain curves compared to older patients. For example, patient 2, a 50-year-old male with a tricuspid aortic valve (TAV), shows a relatively high maximum stress in S1 of 1.14 N/cm² and 3.35 N/cm² in S2. These values are higher than those of patient 1, a 67-year-old female, who shows 0.62 N/cm² in S1 and 2.10 N/cm² in S2. This trend can also be seen in patient 8, a 37-year-old male with TAV, who demonstrates a similarly high stress in S1 of 1.05 N/cm² and 3.18 N/cm² in S2. These differences suggest that younger patients tend to exhibit a higher capacity to withstand stress in both the elastic and plastic regions.

In contrast, older patients, such as patient 6 (74 years old) and patient 7 (76 years old), show varied mechanical responses. Patient 6, a male with TAV, demonstrates a particularly high maximum stress in S1 (1.18 N/cm²) and an even higher value in S2 (3.58 N/cm²), which contradicts the general trend of older patients having lower mechanical strength. This suggests that individual patient variability may play a larger role in influencing the mechanical properties of aneurysmatic aortic tissues, even in older age groups. Patient 7, a male with a bicuspid aortic valve (BAV), shows lower stress values compared to patient 6, with 0.72 N/cm² in S1 and 2.67 N/cm² in S2, but still demonstrates a strain of 3.26 at S3, indicating a relatively high capacity for deformation before rupture. These variations among older patients highlight the complexity of factors influencing aortic tissue mechanics.

Gender also seems to influence mechanical behavior, although the patterns are less clear. The two female patients, patient 1 and patient 9, exhibit lower stress values in both S1 and S2 compared to the male patients. For instance, patient 9, a 56-year-old female with TAV, shows a maximum stress of 0.42 N/cm² in S1 and 1.96 N/cm² in S2, values that are consistently lower than male patients of a similar age, such as patient 10 (53 years old), who demonstrates higher stresses of 0.92 N/cm² in S1 and 2.63 N/cm² in S2. However, patient 9 shows a relatively high strain at S3 (4.46), indicating a higher capacity for elongation at the point of rupture compared to some male patients. This suggests that while female patients may exhibit lower stress resistance, their tissues could have greater elongation potential under certain conditions.

Valve type also seems to have a notable influence on mechanical properties. Patients with BAV, such as patient 7 and patient 11, tend to show higher stresses in the plastic region (S2) compared to some TAV patients. Patient 11, a 55-year-old male with BAV, shows a stress of 2.32 N/cm² in S2, which is lower than some younger TAV patients but still within a relatively high range for a patient of his age. This could indicate that the presence of BAV affects the mechanical properties of the aortic wall, particularly in terms of its response in the plastic region, where deformation becomes irreversible. However, TAV patients such as patient 2 and patient 8 also show high values in both S1 and S2, suggesting that while valve morphology plays a role, other factors such as age and individual tissue variability are likely important contributors.

Special attention should be given to patient 5, a 33-year-old male with Marfan syndrome. His mechanical properties, although comparable to other patients with TAV, must be interpreted differently due to the

underlying connective tissue disorder. In S1, he shows a stress of 0.59 N/cm², similar to that of other patients of his age, and in S2, his stress reaches 2.31 N/cm². However, Marfan syndrome is known to affect the structural integrity of the aortic wall, and the values obtained from this patient likely reflect pathological changes that are not comparable to other patients in this study.

outer													
#	Gender	Age	Valve Type	S1				S2				S3	
				σ (N/cm2)		ε (-)		σ (N/cm2)		ε (-)		ε (-)	
				mean	sd	mean	sd	mean	sd	mean	sd	mean	sd
1	F	67	TAV	0.59	0.26	0.04	0.01	1.75	0.71	0.49	0.12	2.66	0.30
2	M	50	TAV	0.81	0.35	0.07	0.08	2.31	0.47	0.54	0.14	3.01	0.70
3	M	54	TAV	-	-	-	-	-	-	-	-	-	-
5	M	33	TAV	-	-	-	-	-	-	-	-	-	-
6	M	74	TAV	0.54	0.00	0.02	0.00	1.64	0.00	0.28	0.00	3.30	0.00
7	M	76	BAV	0.88	0.33	0.05	0.02	2.50	0.51	0.38	0.09	2.75	1.01
8	M	37	TAV	1.24	1.18	0.11	0.15	3.06	0.84	0.54	0.11	3.18	1.07
9	F	56	TAV	0.61	0.19	0.06	0.06	1.55	0.33	0.64	0.14	2.98	0.83
10	M	53	TAV	0.63	0.13	0.04	0.02	2.21	0.33	0.59	0.20	3.07	1.13
11	M	55	BAV	0.57	0.09	0.05	0.03	2.28	0.54	0.62	0.24	3.94	1.14
12	M	54	TAV	0.73	0.00	0.02	0.00	2.50	0.00	0.56	0.00	4.03	0.00

Table 5: Patient Characteristics and Stress-Strain values for outer incision.

In the outer table, age again plays a significant role in determining the mechanical properties of the aortic tissues. Younger patients tend to exhibit higher maximum stresses in both the elastic and plastic regions. Patient 8, a 37-year-old male with TAV, shows the highest values in the table, with 1.24 N/cm² in S1 and 3.06 N/cm² in S2. These high stress values suggest that the tissues of younger patients have a greater capacity to withstand force before transitioning into the plastic deformation region and before rupture. Comparatively, older patients, such as patient 1 (67 years old) and patient 6 (74 years old), show much lower stress values. For example, patient 1 shows a maximum stress of 0.59 N/cm² in S1 and 1.75 N/cm² in S2, while patient 6 shows even lower values, with 0.54 N/cm² in S1 and 1.64 N/cm² in S2. This trend of decreasing stress resistance with age is consistent with the expected deterioration of the aortic wall's mechanical properties in elderly patients.

The influence of gender is somewhat less pronounced in the outer table compared to the inner table, although it still plays a role. Female patients, such as patient 1 and patient 9, continue to show lower stress values compared to male patients. Patient 1, a 67-year-old female, shows 0.59 N/cm² in S1 and 1.75 N/cm² in S2, while patient 9, a 56-year-old female, shows slightly higher values with 0.61 N/cm² in S1 and 1.55 N/cm² in S2. Despite these lower stress values, female patients demonstrate comparable or even higher strains at the point of rupture (S3). For example, patient 9 shows a strain of 2.98 at S3, which is higher than several male patients in the same age range. This indicates that while female tissues may exhibit lower resistance to stress, they retain a significant ability to stretch before rupture occurs.

Valve type continues to be a differentiating factor in the outer table. Patients with BAV, such as patient 7 and patient 11, show moderately high stress values in both S1 and S2, although these values are not as high as those seen in some younger TAV patients. For instance, patient 7 (76 years old) shows a stress of 0.88 N/cm² in S1 and 2.50 N/cm² in S2, which are relatively high for his age but still lower than the stress values observed in younger TAV patients such as patient 8. Similarly, patient 11 (55 years old) shows a stress of 0.57 N/cm² in S1 and 2.28 N/cm² in S2, demonstrating that while valve type influences mechanical properties, age likely remains the dominant factor in determining overall tissue strength and resistance to deformation.

Again, patient 5 with Marfan syndrome is absent from the outer table, and the mechanical properties of his aortic tissue in this region cannot be directly compared to the other patients. However, given the known effects of Marfan syndrome on the structural integrity of the aorta, it is likely that his results, if available, would further illustrate the distinct pathological alterations in the mechanical behavior of the aortic wall caused by this genetic disorder.

Patients' characteristics influence on thickness

#	Gender	Age	Valve Type	inner			outer		
				twall	tin	tout	twall	tin	tout
1	F	67	TAV	2.28 ± 0.23	0.81 ± 0.10	1.34 ± 0.25	2.32 ± 0.20	1.49 ± 0.20	0.93 ± 0.10
2	M	50	TAV	2.23 ± 0.13	0.84 ± 0.08	1.36 ± 0.15	2.22 ± 0.14	1.51 ± 0.14	0.70 ± 0.07
3	M	54	TAV	2.50 ± 0.19	0.80 ± 0.12	1.63 ± 0.14	2.42 ± 0.17	1.54 ± 0.11	0.79 ± 0.09
5	M	33	TAV	2.32 ± 0.19	0.68 ± 0.07	1.60 ± 0.16	2.30 ± 0.18	1.44 ± 0.12	0.80 ± 0.12
6	M	74	TAV	2.21 ± 0.17	0.73 ± 0.06	1.52 ± 0.14	2.26 ± 0.17	1.47 ± 0.16	0.83 ± 0.09
7	M	76	BAV	2.25 ± 0.17	0.67 ± 0.07	1.54 ± 0.13	2.17 ± 0.25	1.39 ± 0.25	0.80 ± 0.11
8	M	37	TAV	2.12 ± 0.17	0.65 ± 0.07	1.44 ± 0.17	2.14 ± 0.15	1.31 ± 0.14	0.79 ± 0.07
9	F	56	TAV	2.24 ± 0.17	0.70 ± 0.06	1.76 ± 0.21	2.36 ± 0.23	1.48 ± 0.26	0.86 ± 0.09
10	M	53	TAV	2.28 ± 0.24	0.72 ± 0.10	1.54 ± 0.20	2.26 ± 0.12	1.42 ± 0.12	0.81 ± 0.07
11	M	55	BAV	2.15 ± 0.24	0.67 ± 0.06	1.42 ± 0.25	2.14 ± 0.17	1.34 ± 0.17	0.79 ± 0.08
12	M	54	TAV	2.29 ± 0.13	0.74 ± 0.07	1.52 ± 0.19	2.25 ± 0.13	1.40 ± 0.14	0.86 ± 0.11

Table 6: Patient Characteristics and Thickness values for inner and outer incision.

The influence of patient characteristics on the thickness values—total wall thickness, intimal (t_{in}), and adventitial (t_{out}) layers—can be assessed by examining age, valve type, Marfan syndrome, and gender.

Age appears to have a significant impact on the wall thickness measurements. Older patients tend to exhibit thicker vessel walls, particularly in the intimal and adventitial layers. For example, patient 6 (74 years old) shows an inner intimal thickness (t_{in}) of 0.73 ± 0.06 mm, which is thicker than that of younger patients like patient 12 (54 years old), whose tin value is 0.74 ± 0.07 mm. This trend of increased wall thickness with age is seen consistently across other measurements as well, such as the outer adventitial thickness (tout), where older individuals like patient 1 (67 years old) exhibit values of 0.93 ± 0.10 mm compared to younger individuals. These findings suggest that aging may lead to progressive thickening of the intima and adventitia, likely due to vascular remodeling processes.

Valve type is another important factor influencing the thickness values. Patients with bicuspid aortic valve (BAV), such as patients 7 and 11, tend to have thinner intimal layers compared to those with tricuspid aortic valve (TAV). For instance, patient 7 has an inner intimal thickness of 0.67 ± 0.07 mm, which is lower than that of most TAV patients, such as patient 9 (0.70 ± 0.06 mm) or patient 12 (0.74 ± 0.07 mm). The thinner intimal and adventitial layers seen in BAV patients may be related to the distinct hemodynamic forces and structural alterations associated with this valve type, which influence the vessel wall's development and thickness.

It should be noted that patient 5 has Marfan syndrome resulting in distinct thickness patterns. The reduced thickness in both the intimal and adventitial layers (inner tin: 0.68 ± 0.07 mm, outer tout: 0.80 ± 0.12 mm) can be attributed to the structural abnormalities associated with the condition, which affects the integrity and composition of the vessel wall. However, Marfan syndrome represents a specific pathological condition, and its influence on wall thickness should be interpreted within that context.

Gender differences are less clear due to the small sample size of female patients. Only two women (patients 1 and 9) are represented in the dataset, making it challenging to draw definitive conclusions. However, the available data suggest that female patients may exhibit slightly thicker adventitial layers compared to males of similar age. For instance, patient 9 (56 years old) has a higher outer adventitial thickness (tout: 1.76 ± 0.21 mm) than most males in the same age range, such as patient 10 (53 years old) with a tout of 1.54 ± 0.20 mm. Nonetheless, the limited number of female patients restricts the ability to generalize these findings, and further investigation would be necessary to confirm any potential gender-based differences in vessel wall thickness.

In summary, age plays a central role in influencing vessel wall thickness, with older patients generally showing thicker intimal and adventitial layers. Valve type, specifically BAV, tends to be associated with thinner vessel walls, while the presence of Marfan syndrome results in reduced thickness, likely due to connective tissue abnormalities. Gender-related differences in wall thickness are harder to establish due to the small sample size of female patients.

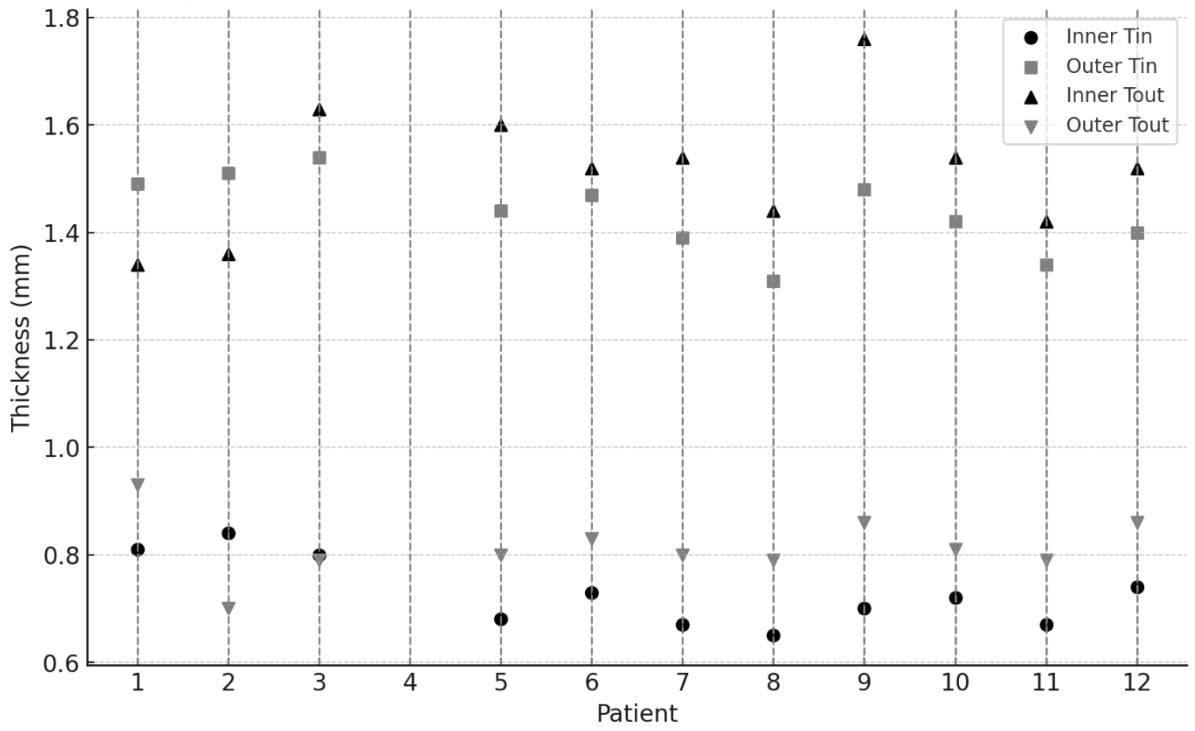

Table 7: Comparison of inner and outer aortic wall thickness across patients

The diagram offers a clear visual representation of the thickness measurements for the inner and outer vessel wall layers across twelve patients, focusing on intimal (t_{in}) and adventitial (t_{out}) contributions. A consistent separation between inner and outer measurements is evident for each patient. Inner t_{in} values, corresponding to the intima in the case of an intima-media incision, are consistently lower than outer t_{in} values, which represent the combined thickness of the intima and media layers. Similarly, inner t_{out}, which includes both the media and adventitia, consistently exceeds outer t_{out}, where only the adventitial layer is reflected. This pattern underscores the structural differences between the layers, confirming that the methodology appropriately distinguishes between these components of the vessel wall.

Notably, the data reveal differences between patients, particularly in the relative gaps between inner and outer thicknesses. For example, older patients, such as patient 1 (67 years old) and patient 6 (74 years old), show relatively larger differences between inner and outer t_{in} and t_{out} values compared to younger patients. This may be attributable to age-related changes in the vessel wall, where the intima tends to thicken progressively with age, contributing to the widening of the gap between inner and outer values. In contrast, younger patients such as patient 8 (37 years old) exhibit smaller differences between inner and outer measurements, suggesting a more uniform contribution of the intima and media to overall vessel thickness at a younger age.

These age-related differences in thickness gaps likely reflect the vascular remodeling processes that occur with aging, where the intima and media layers experience progressive thickening due to increased deposition of extracellular matrix and other structural changes. This gradual thickening can explain why older patients display more pronounced gaps between inner and outer tin and tout measurements.

Discussion

The results of this study demonstrate that specimens with an inner incision, mimicking rupture initiation between the intima and media layers, exhibited higher maximum forces (Fmax) at failure compared to specimens with an outer incision, between the media and adventitia layers. The average Fmax values were higher in the inner incision group, indicating that the inner layers of the aorta possess greater mechanical strength and resistance to rupture than the outer layers. These results align with those of Sommer et al., who reported radial failure stress values of approximately 140.1 ± 15.9 kPa in human abdominal aortas, though the radial tensile strength was lower than in other directions due to the inherent anisotropic properties of the aortic wall. Similarly, Schriefl et al. found radial tensile strength to be 131 ± 56 kPa, reinforcing the notion that the aortic wall's ability to resist mechanical stress in the radial direction is significantly weaker compared to the circumferential or longitudinal directions. This is consistent with the finding in the current study that the outer layers are more susceptible to failure under radial tensile stress, suggesting that once an initial rupture occurs in these regions, it may easily propagate, leading to dissection or aneurysm rupture.

The greater variability in the Fmax values of the outer incision group in this study could be attributed to the structural heterogeneity of the outer layers, as described in the literature. Previous studies have shown that the media-adventitia interface, where rupture typically occurs in dissections, is mechanically weaker due to fewer cohesive forces between lamellae. This variability may reflect the less organized structure of the adventitia, which is primarily composed of collagen fibers that offer less mechanical resistance compared to the elastin and collagen fibers within the media. The results of MacLean et al., who studied porcine thoracic aortas, showed that radial failure stress in the media-adventitia region was significantly lower than in the intima-media region, which aligns with the findings of the current study, indicating that the outer layers are more prone to rupture.

Comparing the force-displacement behavior observed in this study with those reported in the literature further elucidates the differences in mechanical properties across the aortic wall layers. Sommer et al. noted that the aortic media exhibits a linear elastic response followed by a region of damage accumulation, ultimately leading to tissue failure. The current study's force-displacement curves also reflect this mechanical behavior, with the inner layers demonstrating greater resistance to failure. The outer layers, however, displayed a steeper drop-off in force, suggesting a more brittle failure mechanism, which is consistent with findings in atherosclerotic or weakened aortic tissues. The fact that the specimens in this study originated from patients with aneurysms provides further context, as previous research has demonstrated that pathological tissues, particularly those affected by aneurysms, exhibit reduced mechanical strength. For example, Schriefl et al. reported that atherosclerotic specimens fail at significantly lower stresses than healthy tissues due to structural degeneration, a pattern also evident in the present study's results.

When comparing the elastic modulus, the current study found distinct differences between the inner and outer layers, with the inner layers generally showing higher stiffness in the elastic region of deformation. These findings correspond with those of previous studies that have measured radial stiffness in the aortic wall. Sommer et al. reported average radial stiffness values of 559 ± 264 kPa, which, while somewhat lower than circumferential stiffness values, indicate that the aorta maintains considerable resistance to deformation in the radial direction, particularly in the media layer. This study's findings that the inner layers (intima-media) exhibited higher stiffness are consistent with the literature, suggesting that these layers contribute more to the aortic wall's mechanical resilience during the early stages of tensile loading. The outer layers, on the other hand, demonstrated lower elastic modulus values, indicating greater compliance and, thus, a higher susceptibility to early failure. These differences in mechanical behavior between the layers help explain the initiation and progression of aortic dissection, which typically occurs in regions of reduced stiffness, such as the media-adventitia interface.

The influence of patient-specific characteristics on the mechanical properties of the aortic wall is also a critical aspect of the discussion. Previous research has emphasized the importance of considering patient demographics, such as age, gender, and valve morphology, when evaluating aortic mechanics. Pasta et al., for example, found that patients with bicuspid aortic valves (BAV) tend to exhibit lower delamination strength compared to those with tricuspid aortic valves (TAV), a finding consistent with the present study's results. In this study, patients with BAV showed lower mechanical resistance in both the elastic and plastic regions of deformation, suggesting that

the altered hemodynamics associated with BAV may predispose these individuals to earlier or more severe structural weakening of the aortic wall. This could explain why BAV patients are at higher risk for aortic dissection and rupture. The literature supports this, with studies showing that BAV leads to increased mechanical stress on the aortic wall, contributing to its progressive deterioration.

Age-related differences in mechanical properties are also supported by existing research. In the current study, younger patients generally exhibited higher stress values in both the elastic and plastic regions compared to older patients. This finding is consistent with previous studies, such as those by Pasta et al., which demonstrated that younger aortic tissues have a greater capacity to withstand mechanical stress. The progressive stiffening and thickening of the aortic wall with age, as shown by increased wall thickness in older patients, leads to reduced mechanical strength and elasticity, as evidenced by lower Fmax and higher susceptibility to rupture. The literature also supports the notion that aging leads to the accumulation of microstructural defects, such as collagen cross-linking and elastin degradation, which reduce the mechanical resilience of the aortic wall.

Additionally, gender differences in mechanical properties observed in this study, though not as pronounced, align with some findings in the literature. Studies such as those by Pasta et al. have reported lower mechanical strength in female aortic tissues compared to male tissues, which was also observed in the current study. While the sample size of female patients in this study was small, the results suggest that female aortic tissues may be more prone to rupture under tensile loading. This could be due to hormonal influences or differences in the structural composition of the aortic wall between men and women, as proposed in previous research.

One of the strengths of this study is its focus on a detailed mechanical analysis of different anatomical regions of the aorta, providing insights into how rupture initiation and propagation vary depending on location. The finding that the posterior region exhibited the highest mechanical resistance, while the left lateral and anterior regions were more vulnerable, aligns with previous studies that have reported regional variations in aortic mechanics. The literature suggests that differences in hemodynamic forces, such as blood flow and pressure, across the aortic wall may contribute to these regional differences. Schriefl et al. noted that the posterior region of the aorta tends to be more robust due to the structural organization of collagen and elastin fibers, which may help explain the higher mechanical strength observed in this region in the current study.

In terms of limitations, the current study's relatively small sample size, particularly in some anatomical regions, may affect the generalizability of the findings. Additionally, while the mechanical tests provide valuable insights into the tensile properties of the aortic wall, they do not capture the underlying microstructural changes that contribute to the observed behavior. Integrating histological analyses, as suggested by previous studies, would offer a more complete understanding of how structural factors such as fiber alignment and the presence of microdefects influence mechanical performance. Future studies could expand on this work by combining mechanical testing with histological and imaging techniques to further explore the relationship between microstructure and mechanical behavior in the aneurysmatic aortic wall.

Conclusion

This study aimed to investigate the mechanical properties of the aneurysmatic ascending aorta through direct tension testing in the radial direction, focusing on rupture propagation and comparing the mechanical behaviors of different anatomical regions of the aortic wall. The study was designed to examine how the inner (intima-media) and outer (media-adventitia) layers respond to mechanical stress, both in terms of failure mechanisms and tissue resilience, with the ultimate objective of better understanding rupture initiation and propagation in the context of aortic disease. Through the analysis of force-displacement curves, mechanical parameters such as maximum force (F_{max}), yield force (F_{yield}), strain, elastic modulus, and peak elastic modulus (PEM) were obtained for each anatomical region and layer, providing a detailed characterization of the mechanical behavior of the aortic wall.

The research successfully achieved its primary objectives by offering new insights into how different regions and layers of the aneurysmatic ascending aorta respond to radial tensile forces. The key finding that the inner layers, particularly at the intima-media interface, exhibit greater mechanical strength and resistance to rupture compared to the outer layers, which include the media-adventitia interface, is of significant clinical relevance. This observation was consistent across most regions of the aorta and aligns with previous findings in the literature, which have noted the mechanical importance of the intima-media boundary. The study confirmed that the outer layers are more vulnerable to rupture propagation. The higher mechanical variability observed in specimens with outer incisions also points to the structural heterogeneity of the adventitia, which is consistent with previous studies that have shown this layer to be less organized and less resistant to tensile forces than the more cohesive intima-media interface.

Furthermore, the study provided important insights into regional variations within the aortic wall, demonstrating that certain regions, such as the posterior and right lateral areas, exhibit higher mechanical strength compared to more vulnerable regions like the anterior and left lateral areas. This finding suggests that the structural integrity of the aorta may differ depending on its anatomical location, which could have significant implications for understanding the localized development of aneurysms and the propensity for rupture in specific regions of the aortic wall. The posterior region, in particular, was found to be more resistant to tensile forces, which supports the idea that the structural composition of this region provides it with greater mechanical resilience. This regional variation in mechanical properties, as observed in the current study, adds an important dimension to our understanding of aortic biomechanics and highlights the need for region-specific analyses when assessing rupture risks in patients with aortic disease.

The results of this study contribute significantly to the body of knowledge on the mechanical properties of the aneurysmatic ascending aorta, particularly in the context of radial tensile testing. While previous studies have provided valuable data on the circumferential and longitudinal mechanical properties of the aortic wall, this study focuses on the radial direction, which is crucial for understanding rupture propagation between the layers of the aorta. By examining the mechanical behavior of the intima-media and media-adventitia interfaces separately, this study provides a clearer picture of how different layers of the aortic wall contribute to its overall mechanical stability. The findings that the inner layers are mechanically stronger and more resistant to failure than the outer layers offer important insights into the mechanisms of aortic dissection, which often propagate through the media-adventitia interface. This knowledge is critical for improving clinical assessments of rupture risk and for informing surgical strategies aimed at reinforcing the vulnerable outer layers of the aorta.

The broader implications of this research extend to the clinical management of aortic aneurysms and dissections. Understanding the layer-specific and region-specific mechanical vulnerabilities of the aortic wall can help clinicians identify patients who are at higher risk for rupture and target interventions more effectively. For example, patients with aneurysms in regions that exhibit lower mechanical strength, such as the anterior or left lateral areas, may require closer monitoring or earlier surgical intervention. Similarly, patients with BAV, who are known to have lower mechanical resistance in the aortic wall, may benefit from more aggressive treatment strategies to prevent rupture. The study's findings also suggest that patient-specific factors, such as age and valve morphology, play a critical role in determining mechanical behavior, further underscoring the need for personalized approaches to the management of aortic disease.

References

[1] “"OLI - Drawing Parts of aorta in relation to heart and diaphragm - English labels" by Open Learning Initiative, license: CC BY-NC-SA”.

[2] L. F. Hiratzka, G. L. Bakris, J. A. Beckman and et al, “2010 ACCF/AHA/AATS/ACR/ASA/SCA/SCAI/SIR/STS/SVM guidelines for the diagnosis and management of patients with Thoracic Aortic Disease: a report of the American College of Cardiology Foundation/American Heart Association Task Force on Practice Guidelines, A,” *Circulation,* vol. 121, no. 13, pp. 266-369, 2010.

[3] N. J. Swerdlow, W. W. Wu and M. L. Schermerchorn, “Open and Endovascular Management of Aortic Aneurysms,” *Circulation Research,* vol. 124, no. 4, 2019.

[4] J. Collegde, “Abdominal aortic aneurysm: update on pathogenesis and medical treatments,” *Nat. Rev. Cardiol.,* vol. 16, pp. 225-242, 2019.

[5] G. Qian, O. Adeyanju, A. Olayuyin and X. Guo, “Abdominal aortic aneurysm for mation with a focus on vascular smooth muscle cells,” *Life,* vol. 12, p. 191, 2022.

[6] L. B. Granville, D. J. Colledge and Z. Kassiri, “Pathogenic mechanisms and the potential of drug therapies for aortic aneurysm,” *Am. J. Physiol. Heart Circ. Physiol.,* vol. 318, pp. 652-670, 2020.

[7] J. Gao and et al, “The mechanism and therapy of aortic aneurysms,” *Signal Transduct. Target. Ther.,* vol. 8, p. 55, 2023.

[8] M. J. Cho, M.-R. Lee and J.-G. Park, “Aortic aneurysms: current pathogenesis and therapeutic targets,” *Experimental & Molecular Medicine,* vol. 55, pp. 2519-2530, 2023.

[9] H. Lu and A. Daugherty, “Aortic Aneurysms,” *Arteriosclerosis, Thrombosis, and Vascular Biology,* pp. 59-65, 2017.

[10] F. Cikach, M. Y. Desai, E. Roselli and V. Kalahasti, “Thoracic aortic aneurysm: How to counsel, when to refer,” *CLEVELAND CLINIC JOURNAL OF MEDICINE,* vol. 85, no. 6, 2018.

[11] C. Olsson, S. Thelin, E. Stahle, A. Ekbom and F. Granath, “ Thoracic aortic,” *Circulation,* vol. 114, no. 24, pp. 2611-2618, 2006.

[12] W. Clouse, J. Hallet and H. Schaff , “Acute aortic dissection: population-based incidence compared with degenerative aortic aneurysm rupture,” *Mayo Clinic Proceedings,* vol. 79, no. 2, pp. 176-180, 2004.

[13] “Centers For Disease Control and Prevention,” 27 September 2021. [Online]. Available: https://www.cdc.gov/heartdisease/aortic_aneurysm.html.

[14] K. Cheung, M. Boodhwani, K.-L. Chan, L. Beauchesne, A. Dick and T. Coutinho, “Thoracic Aortic Aneurysm Growth: Role of Sex and Aneurysm Etiology,” *American Heart Association,* 2017.

[15] G. Kuzmik, A. Sang and J. Eleftheriades, “ Natural history of thoracic aortic,” *Journal of Vascular Surgery,* vol. 56, pp. 565-571, 2012.

[16] R. Davies, L. Goldstein, M. Coady, S. Tittle, J. Rizzo, G. Kopf and J. Eleftheriades, “Yearly rupture or dissection rates for thoracic aortic aneurysms: simple,” *The Annals of Thoracic Surgery,* vol. 73, pp. 17-27, 2002.

[17] R. Davies, A. Gallo, M. Coady, G. Tellides, D. Botta, B. Burke, M. Coe, G. Kopf and J. Eleftheriades, “Novel measurement of relative aortic size predicts rupture,” *The Annals of Thoracic Surgery,* vol. 81, pp. 169-177, 2006.

[18] T. K. M. Wang and M. Y. Desai, “Thoracic aortic aneurysm: Optimal surveillance and treatment,” *CLEVELAND CLINIC JOURNAL OF MEDICINE ,* vol. 87, no. 9, pp. 557-568, 2020.

[19] L. Svensson, K. Kim, E. Blackstone and et al., “Bicuspid aortic valve surgery with proactive ascending aorta repair,” *Thorac Cardiovasc Surg,* vol. 142, pp. 622-9, 2011.

[20] N. Tzemos, J. Therrien, J. Yip and e. al., “Outcomes in adults with bicuspid aortic valves,” *JANA,* vol. 300, pp. 1317-25, 2008.

[21] M. A. Coady, R. R. Davies, M. Roberts and et al, “Familial patterns of thoracic aortic aneurysms,” *Arch Surg,* vol. 134, no. 4, pp. 361-367, 1999.

[22] H. de Beaufort, S. Trimarchi, A. Korach, M. Di Eusanio, D. Gilon, D. Montgomery, A. Evangelista, A. C. Braverman, E. P. Chen, E. M. Isselbacher, T. G. Gleason, C. De Vincentis, T. M. Sundt, H. J. Patel and K. A. Eagle, “Aortic dissection in patients with Marfan syndrome based on the IRAD data,” *Annals of Cardiothoracic Surgery,* vol. 6, no. 6, 2017.

[23] M. E. Senser, S. Misra and S. Henkin, “Thoracic Aortic Aneurysm: A Clinical Review,” *Cardiology Clinics,* vol. 39, no. 4, pp. 505-515, 2021.

[24] “Cardiovascular manifestations of hypermobile Ehlers–Danlos syndrome and hypermobility spectrum disorders,” *Society for vascular Medicine,* vol. 27, no. 3, 2022.

[25] A. Lin, B. Lippe and R. Rosenfeld, “Further delineation of aortic dilation, dissection, and rupture in patients with Turner syndrome,” *Pediatrics,* vol. 102, no. 12, 1998.

[26] V. Sybert and E. McCauley, “Turner's syndrome,” *N Engl J Med,* vol. 351, pp. 1227-38, 2004.

[27] M. Mahboob, P. Rout, S. W. Leslie and S. R. A. Bokhari, Autosomal Dominant Polycystic Kidney Disease, Treasure Island (FL): StatPearls Publishing, 2024.

[28] P.-H. Sung, Y.-H. Yang, H.-J. Chiang, J. Y. Chiang, C.-T. Liu, C.-M. Yu and H.-K. Yip, “Risk of aortic aneurysm and dissection in patients with autosomal-dominant polycystic kidney disease: a nationwide population-based cohort study,” *Oncotarget,* vol. 8, no. 34, pp. 57594-57604, 2017.

[29] M. T. Greally, Shprintzen-Goldberg Syndrome, Seattle (WA): Adam MP, Feldman J, Mirzaa GM, et al., editors., 1993-2024.

[30] “National Institute of Arthritis and Musculoskeletal and Skin Diseases, "Takayasu's Arteritis,",” [Online]. Available: https://www.niams.nih.gov/.

[31] “Mayo Clinic, "Giant Cell Arteritis,",” [Online]. Available: https://www.mayoclinic.org/.

[32] “Johns Hopkins Medicine, "Behcet's Disease,",” [Online]. Available: https://www.hopkinsmedicine.org/.

[33] “Cleveland Clinic, "Ankylosing Spondylitis,",” [Online]. Available: https://my.clevelandclinic.org/.

[34] “American Heart Association, "Mycotic Aneurysms,",” [Online]. Available: https://www.heart.org/.

[35] “Centers for Disease Control and Prevention, "Syphilis,",” [Online]. Available: https://www.cdc.gov/.

[36] “MedlinePlus, "Aortic Aneurysm,",” [Online]. Available: https://medlineplus.gov/.

[37] C. A. Della and et al, “Prevention of thoracic aortic aneurysm and dissection: genetic and molecular determinants.,” *Annals of Thoracic Surgery,* vol. 83, pp. 3-9, 2007.

[38] M. W. Majesky, “Developmental basis of vascular smooth muscle diversity.,” *Arteriosclerosis, Thrombosis, and Vascular Biology,* vol. 6, pp. 1248-1258, 2007.

[39] S. Malekis and et al, “Mesenchymal state of intimal cells may explain higher propensity to ascending aortic aneurysm in bicuspid aortic valves,” *Scientific Reports,* vol. 6, 2016.

[40] A. Sayed, M. Munir and E. I. Bahbah, “Aortic Dissection: A Review of the Pathophysiology, Management and Prospective Advances,” *Current Cardiology Reviews,* vol. 17, 2021.

[41] S. Trimarchi, C. A. Nienaber, V. Rampoldi, T. Myrmel, T. Suzuki and et al, “Contemporary results of surgery in acute type A aortic dissection: the International Registry of Acute Aortic Dissection experience,” *J Thorac Cardiovasc Surg,* vol. 129, pp. 112-22, 2005.

[42] K. Krishnan, L. Ge, H. Haraldsson, M. D. Hope, D. A. Saloner, J. M. Guccione and E. E. Tseng, “Ascending thoracic aortic aneurysm wall stress analysis using patient-specific finite element modeling of in vivo magnetic resonance imaging,” *Interactive CardioVascular and Thoracic Surgery,* vol. 21, pp. 471-480, 2015.

[43] A. M. Mansour, S. Peters, M. A. Zafar, J. A. Rizzo and et al, “Prevention of Aortic Dissection Suggests a Diameter Shift to a Lower Aortic Size Threshold for Intervention,” *Cardiology,* vol. 139, pp. 139-146, 2018.

[44] B. A. Ziganshin, M. A. Zafar and J. A. Eleftheriades, “Descending threshold for ascending aortic aneurysmectomy: Is it time for a “left-shift” in guidelines?,” *J. Thorac. Cardiovasc. Surg.,* vol. 157, pp. 37-42, 2019.

[45] K. Monaghan, F. Orelaru, A. Naeem, R. A. Ahmad and et al, “Should We Operate on Thoracic Aortic Aneurysm of 5-5.5cm in Bicuspid Aortic Valve Disease Patients?,” *Cardiol. Cardiovasc. Med.,* vol. 5, pp. 651-662, 2021.

[46] R. R. Davies, A. Gallo, M. A. Coady, G. Tellides and et al, “Novel measurement of relative aortic size predicts rupture of thoracic aortic aneurysms,” *Ann. Thorac. Surg.,* vol. 81, pp. 169-177, 2006.

[47] K. K. Tiwari, S. Bevilacqua, G. D. Aquaro, P. Festa and et al, “Function Magnetic Resonance Imaging in the Evaluation of the Elastic Properties of Ascending Aortic Aneurysm,” *Braz. J. Cardiovasc. Surg.,* vol. 24, no. 451-457, 2019.

[48] J. Wu, M. A. Zafar, Y. Li, A. Saeyeldin, Y. Huang and et al, “Ascending aortic length and risk of aortic adverse events: The neglected dimension,” *J. Am. Coll. Cardiol.,* vol. 74, pp. 1883-1894, 2019.

[49] G. Zemtsovskaja, K. Pilt, A. Samarin, J. Abina, K. Meigas and M. Viigimaa, “Construction of gender-specific regression models for aortic length estimation based on computed tomography images,” *Health Technol.,* vol. 10, pp. 679-687, 2020.

[50] N. D. Anfinogenova, V. E. Sinitsyn, B. N. Kozlov, D. S. Panfilov, S. V. Popov, A. V. Vrublevsky, A. Chernyavsky, T. Bergen, V. V. Khovrin and W. Y. Ussov, "Existing and Emerging Approaches to Risk Assessment in Patients with Ascending Thoracic Aortic Dilatation," *Journal of Imaging,* vol. 8, no. 280, 2022.

[51] A. Ghulam , L. Fusini, A. Dalla Cia, G. Tamborini, P. Gripari, M. Muratori, M. E. Mancini and et al, "Technological advancements in echo-cardiographic assessment of thoracic aortic dilatation: Head to head comparison among multidetector computed tomography, 2-dimensional, and 3-dimensional echocardiography measurements," *J. Thorac. Imaging,* vol. 33, pp. 232-239, 2018.

[52] K. E. Boczar, M. Boodhwani, L. Beauchesne, C. Dennie and et al, "Aortic Stiffness, Central Blood Pressure, and Pulsatile Arterial Load Predict Future Thoracic Aortic Aneurysm Expansion," *Hypertension,* vol. 77, pp. 126-134, 2021.

[53] S. Parikh, B. Ganizada, G. Debeij and et al, "Intra-Operative Video-Based Measurement of Biaxial Strains of the Ascending Thoracic Aorta," *Biomedicines,* vol. 9, p. 670, 2021.

[54] "Computational evaluation of mechano-elastic properties and of paramagnetic contrast enhancement of thoracic aortic wall in acute myocardial infarction and in non-coronarogenic myocardial damage, from the data of dynamic ECG-gated MRI(MR-elastometry)," *Transl. Med. = Trans. Med.,* vol. 8, pp. 43-58, 2021.

[55] A. Saeyeldin, M. A. Zafar, L. A. Baldassarre and et al, "Aortic delamination-a possible precursor of impending catastrophe," *Int. J. Angiol.,* vol. 30, pp. 160-164, 2021.

[56] I. Vilacosta, P. Aragoncillo, V. Canadas, J. A. San Roman , J. Ferreiros and E. Rodriguwz, "Acute aortic syndrome: a new look at an old conundrum.," *Postgrad Med J.,* vol. 86, no. 1011, pp. 52-61, 2010.

[57] T. Ishii and N. Asuwa, "Collagen and elastin degradation by matrix metalloproteinases and tissue inhibitors of matrix metalloproteinase in aortic dissection," *Hum. Pathol.,* vol. 6, pp. 640-6, 2000.

[58] F. Del Porto, C. di Gioia, L. Tritapepe, L. Feri, M. Leopizzi, I. Nofroni and et al, "The multitasking role of macrophages in Stanford type A acute aortic dissection," *Cardiology,* vol. 127, no. 2, pp. 123-9, 2014.

[59] A. W. Hahn, U. Jonas, F. R. Bulher and T. J. Resink, "Activation of human peripheral monocytes by angiotensin II," *FEBS Lett,* vol. 347, no. 2-3, pp. 178-80, 1994.

[60] J. Gawinecka, F. Schonrath and A. von Eckardstein, "Acute aortic dissection: pathogenesis, risk factors and diagnosis," *Swiss Medical Weekly,* vol. 147, no. 14489, 2017.

[61] M. Khayat, K. J. Cooper, M. S. Khaja, R. Gandhi, Y. C. Bryce and D. M. Williams, "Endovascular management of acute aortic dissection," *Cardiovascular Diagnosis and Therapy,* vol. 8, pp. 97-107, 2018.

[62] D. M. Willians, D. Y. Lee, B. H. Hamilton and et al, "The dissected aorta: part III. Anatomy and radiologic diagnosis of branch- vessel compromise," *Radiology,* vol. 203, pp. 37-44, 1997.

[63] P. G. Hagan, C. A. Nienaber, E. M. Isselbacher and et al, "The International Registry of Acute Aortic Dissection (IRAD): new insights into an old disease," *JAMA,* vol. 283, pp. 897-903, 2000.

[64] J. E. Cigarroa, E. M. Isselbacher, R. W. DeSanctis and et al, "Diagnostic imaging in the evaluation of suspected aortic dissection. Old standards and new directions," *N Engl J Med,* vol. 328, pp. 35-43, 1993.

[65] a. Evagelista, E. M. Isselbacher, E. Bossone and et al, "Insights from the international registry of acute aortic dissection: A 20-year experience of collaborative clinical research," *Circulation,* vol. 137, no. 17, pp. 1846-60, 2018.

[66] A. J. Lovy, E. Bellin, J. M. Levsky, D. Esses and L. B. Haramati, “Prelimiary development of a clinical decision rule for acute aortic syndromes,” *Am J Emerg Med,* vol. 31, no. 11, pp. 1546-1550, 2013.

[67] B. J. Doyle, A. J. Cloonan, M. T. Walsh, D. A. Vorp and T. M. McGloughlin, “Identification of rupture locations in patient-specific abdominal aortic aneurysms using experimental and computational techniques,” *J. Biomech.,* vol. 43, pp. 1408-1416, 2010.

[68] D. P. Nathan, C. Xu, J. H. Gorman III and et al, “Pathogenesis of acute aortic dissection: a finite element stress analysis,” *Ann. Thorac. Surg.,* vol. 91, pp. 458-463, 2011.

[69] “Heterogeneity of tensile strength and matrix metalloproteinase activity in the wall of abdominal aortic aneurysms,” *J. Endovasc. Ther.,* vol. 11, pp. 494-502, 2004.

[70] J. P. Vande Geest, D. Wang, S. R. Wisniewski and et al, “Towards a noninvasive method for determination of patient-specific wall strength distribution in abdominal aortic aneurysms,” *Ann. Biomed. Eng.,* vol. 34, pp. 1098-1106, 2006.

[71] A. Duprey, O. Trabelsi, M. Vola, J. P. Favre and S. Avril, “Biaxial rupture properties of ascending thoracic aortic aneurysms,” *Acta Biomater.,* vol. 42, pp. 273-285, 2016.

[72] S. Sherifova and G. A. Holzapfel, “Biomechanics of aortic wall failure with a focus on dissection and aneurysm: A review,” *Acta Biomater,* vol. 99, pp. 1-17, 2019.

[73] F. M. Davis, A. Daugherty and H. S. Lu, “Updates of Recent Aortic Aneurysm Research,” *Arteriosclerosis, Thrombosis, and Vascular Biology (ATVB),* vol. 39, no. 3, pp. 83-90, 2019.

[74] C. Ye, G. Chang, S. Li, Z. Hu, C. Yao, W. Chen, X. Li and S. Wang, “Endovascular stent-graft treatment for Stanford type A aortic dissection,” *Eur. J. Vasc. Endovasc. Surg.,* vol. 42, pp. 787-794, 2011.

[75] “Thoracic endovascular aortic repair (TEVAR) in proximal (type A) aortic dissection: Ready for a broader application?,” *J. Thorac. Cardiovasc. Surg.,* vol. 153, pp. S3-S11, 2017.

[76] X. Yuan, A. Mitsis and C. A. Nienaber, “Current Understanding of Aortic Dissection,” *Life,* vol. 12, no. 1606, 2022.

[77] X. Yuan, A. Mitsis, T. Semple, M. Castro Verdes and et al, “False lumen intervention to promote remodelling and thrombosis-The FLIRT concept in aortic dissection,” *Catheter. Cardiovasc. Interv,* vol. 92, pp. 732-740, 2018.

[78] G. Meinlschmidt, D. Berdajs and et al, “Perceived Need for Psychosocial Support After Aortic Dissection: Cross-Sectional Survey,” *J. Adv. Nurs.,* vol. 75, pp. 2834-2844, 2019.

[79] M. Jonsson, S. K. Berg, M. Missel and et al, “Am I going to die now? Experiences of hospitalisation and subsequent life after being diagnosed with aortic dissection,” *Scandinavian Journal of Caring Sciences,* vol. 35, no. 3, pp. 929-936, 2021.

[80] E. Sbarouni, P. Georgiadou, M. Manavi and et al, “Long-term outcomes and quality of life following acute type A aortic dissection,” *Hellenic Journal of Cardiology,* vol. 62, no. 6, pp. 463-465, 2021.

[81] N. Ilonzo, E. Taubenfeld, M. D. Yousif, C. Henoud, J. Howitt, M. Wohlauer, M. D'Oria and G. MacCarrick, “The mental health impact of aortic dissection,” *Seminars in Vascular Surgery,* vol. 35, pp. 88-99, 2022.

[82] A. L. Ai, D. Hall and T. N. Pargament Tice, “Posttraumatic growth in patients who survived cardiac surgery: the predictive and mediating roles of faith-based factors,” *J Behav Med,* vol. 36, pp. 186-98, 2013.

[83] J. P. Pirruccello, J. T. Ramo, S. H. Choi and et al, “The Genetic Determinants of Aortic Distention,” *J. Am. Coll. Cardiol.,* vol. 81, pp. 13201-1335, 2023.

[84] H. Wolinsky, “Comparison of medial growth of human thoracic and abdominal aortas,” *Circ. Res.,* vol. 27, pp. 531-538, 1970.

[85] “Comparison of abdominal and thoracic aortic medial structure in mammals. Deviation of man from the usual pattern,” *Circ. Res.,* vol. 25, pp. 677-686, 1969.

[86] C. R. T. di Gioia, A. Ascione, R. Carletti and C. Giordano, “Thoracic Aorta: Anatomy and Pathology,” *Diagnostics,* vol. 13, no. 13, 2023.

[87] D. P. Sokolis and D. C. Iliopoulos, “Impaired mechanics and matrix metalloproteinases/inhibitors expression in female ascending thoracic aortic aneurysms,” *J. Mech. Behav. Biomed. Mater. ,* vol. 34, pp. 154-164, 2014.

[88] J. M. Clark and S. Glagov, “Transmural organization of the arterial media.The lamellar unit revisited,” *Arteriosclerosis,* vol. 5, pp. 19-34, 1985.

[89] G. Koullias, R. Modak, M. Tranquilli, D. P. Korkolis, P. Barash and J. A. Eleftheriades, “Mechanical deterioration underlies malignant behaviorof aneurysmal human ascending aorta,” *J Thorac Cardiovasc Surg,* vol. 130, pp. 677-683, 2005.

[90] J. Biasetti, F. Hussain and T. C. Gassr, “Blood flow and coherent vortices in the normal and aneurysmatic aortas: a fluid dynamical approach to intra-luminal thrombus formation,” *J R Soc Interface,* vol. 8, pp. 1449-1461, 2011.

[91] B. L. Langille, “Arterial remodeling: relation to hemodynamics,” *Can J Physiol Pharmacol,* vol. 74, pp. 834-841, 1996.

[92] R. Mahadevia, A. J. Barker, S. Schnell and et al, “Bicuspid aortic cusp fusion morphology alters aortic three-dimensional outflow patterns, wall shear stress, and expression of aortopathy,” *Circulation,* vol. 129, pp. 673-682, 2014.

[93] S. Farthing and P. Peronneau, “Flow in the thoracic aorta,” *Cardiovasc Res,* vol. 13, pp. 607-20, 1979.

[94] M. M. Bissel, A. T. Hess, L. Biasiolli and et al, “Aortic dilation in bicuspid aortic valve disease: flow pattern is a major contributor and differs with valve fusion type,” *Circ Cardiovasc Imaging,* vol. 6, pp. 499-507, 2013.

[95] G. Sommer, C. T. Gasser, P. Regitnig, M. Auer and G. A. Holzapfel, “Dissection properties of the human aortic media: an experimental study,” *J Biomech Eng.,* vol. 130, no. 2, 2008.

[96] N. F. MacLean, N. L. Dudek and M. R. Roach, “The role of radial elastic properties in the development of aortic dissections,” *J Vasc Surg.,* vol. 29, no. 4, pp. 703-710, 1999.

[97] G. A. Holzapfel, T. C. Gasser and R. W. Ogden, “A new constitutive framework for arterial wall mechanics and a comparative study of material models.,” *Journal of Elasticity,* vol. 61, no. 1-3, pp. 1-48, 2005.

[98] G. Sommer, A. J. Schriefl, G. Zeindlinger, A. Katzensteiner, H. Ainödhofer, A. Saxena and G. A. Holzapfel, “Mechanical properties of human aortas including the descending, abdominal, and thoracic aorta.,” *Journal of Biomechanics,* vol. 41, no. 9, pp. 2036-2042, 2008.

[99] A. J. Schriefl, G. Zeindlinger, D. M. Pierce, P. Regitnig and G. A. Holzapfel, "Determination of the layer-specific distributed collagen fibre orientations in human thoracic and abdominal aortas and common iliac arteries," *J R Soc Interface,* vol. 9, no. 71, pp. 1275-86, 2012.

[100] G. Sommer, S. Sherifova, P. J. Oberwalder, O. E. Dapunt, P. A. Ursomanno, A. DeAnda, B. E. Griffith and G. A. Holzapfel, "Mechanical strength of aneurysmatic and dissected human thoracic aortas at different shear loading modes," *J Biomech,* vol. 49, no. 12, pp. 2374-2382, 2016.

[101] S. Pasta, J. Phillippi, T. Gleason and D. Vorp, "Effect of aneurysm on the mechanical dissection properties of the human ascending thoracic aorta," *The Journal of Thoracic and Cardiovascular Surgery,* vol. 143, no. 2, pp. 460-467, 2012.

[102] G. Sommer, P. Regitnig, L. Koltringer and G. A. Holzapfel, "Biaxial mechanical properties of intact and layer-dissected human carotid arteries at physiological and supraphysiological loadings.," *American Journal of Physiology-Heart and Circulatory Physiology,* vol. 298, no. 3, pp. 898-912, 2012.

[103] D. P. Sokolis, E. M. Kefaloyannis, M. Kouloukoussa, E. Marinos, H. Boudoulas and P. E. Karayannacos, "A structural basis for the aortic stress-strain relation in uniaxial tension," *J Biomech,* vol. 39, no. 9, pp. 1651-62, 2006.

[104] V. A. A. Santamaria, M. F. Garcia, J. Molimard and S. Avril, "Characterization of chemoelastic effects in arteries using digital volume correlation and optical coherence tomography," *Acta Biomater,* vol. 102, pp. 127-137, 2020.

[105] J. Tong, G. Sommer, P. Regitnig and G. Holzapfel, "Dissection Properties and Mechanical Strength of Tissue Components in Human Carotid Bifurcations," *Annals of Biomedical Engineering,* vol. 39, no. 6, pp. 1703-1719, 2011.

[106] N. F. MacLean, M. Dudek and M. R. Roach, "he role of radial tensile tests in understanding the dissection properties of porcine thoracic aortas.," *Journal of Biomechanics,* vol. 41, no. 11, pp. 2462-2468, 2008.

[107] C. Martin, W. Sun, T. Pham and J. A. Elefteriades, "Biomechanical properties of ruptured versus electively repaired ascending aortic aneurysm tissue.," *Annals of Thoracic Surgery,* vol. 95, no. 6, pp. 2067-2073, 2013.

[108] T. Adeniji, "Physiopedia," [Online]. Available: https://www.physiopedia.com/images/thumb/b/b7/Stress-Strain_Curve.jpg/519px-Stress-Strain_Curve.jpg.

[109] Y. Wang, I. S. Panicker, J. Anesi, O. Sargisson, B. Atchison and A. J. R. Habenicht, "Animal Models, Pathogenesis, and Potential Treatment of Thoracic Aortic Aneurysm," *International Journal of Molecular Sciences,* vol. 25, no. 901, 2024.

[110] J. Z. Goldfinger, J. L. Halperin, M. L. Marin, A. S. Stewart, K. A. Eagle and V. Fuster, "Thoracic Aortic Aneurysm and Dissection," *Journal of the American College of Cardiology,* vol. 64, no. 16, 2014.

[111] R. A. Quintana and W. R. Taylor, "Introduction to the Compendium on Aortic Aneurysms," *Circ Res.,* vol. 124, no. 4, pp. 470-471, 2019.

[112] C. R. Smith, S. C. Stamou, R. L. Hooker and et al, "Stentless root bioprosthesis for repair of acute type A aortic dissection," *J Thorac Cardiovasc Surg,* vol. 145, pp. 1540-4, 2013.

[113] T. E. David, S. Armstrong, C. Manlhiot and et al, "Long-term results of aortic root repair using the reimplantation technique," *J Thorac Cardiovasc Surg,* vol. 145, pp. S22-25, 2013.

[114] R. Rolph, J. M. Duffy, B. Modarai and et al, “Stent graft types for endovascular repair of thoracic aortic aneurysms.,” *Cochrane Database Syst Rev,* vol. 3, 2013.

[115] I. Abraha, C. Romagnoli, A. Montedori and et al, “Thoracic stent graft versus surgery for thoracic aneurysm,” *Cochrane Database Syst Rev,* vol. 1, 2009.